Bachelor's Thesis

Biotechnology and Food technology

Biotechnology

2012

Karlo Villa

LOW-ETHANOL SILICA SOLS FOR CELL ENCAPSULATION

TURUN AMMATTIKORKEAKOULU
TURKU UNIVERSITY OF APPLIED SCIENCES

BACHELOR´S THESIS | ABSTRACT
TURKU UNIVERSITY OF APPLIED SCIENCES

Biotechnology and Food technology | Biotechnology

12.6.2012 | Total number of pages 78

Instructor: Mika Jokinen, Principal Lecturer

Karlo Villa

LOW-ETHANOL SILICA SOLS FOR CELL ENCAPSULATION

3D cell encapsulation is a method utilized in the fields of cell biology and tissue engineering and in the testing of chemicals. A variety of materials are available for use as encapsulation matrices. Materials of biological origin feature advantages in terms of biological compatibility but they may feature variations in quality. Synthetic materials can offer higher reproducibility but they may also require modification to achieve the necessary functionalities. One category of synthetic cell encapsulation materials are synthetic silica sols and gels.

Synthetic silica sols and gels can be manufactured via acid catalyzed hydrolysis of silicon alkoxides and base catalyzed condensation of silica aggregates. In the case of tetraethoxysilane (TEOS) a byproduct of the process is ethanol which is harmful for some cell types and it is thus necessary to remove it prior to use in cell encapsulation. The aim of this thesis was to develop a process for producing low-ethanol silica sols and gels for cell encapsulation research.

An evaporation process was developed for removing ethanol from a silica sol produced via the acid catalyzed pathway. In addition, two methods, dry weight determination and an absorbance measurement were applied for studying the properties of sols and gels. The ethanol concentration of the silica sols and gels was determined by headspace gas chromatography. Process development was conducted by adjusting process duration between separate production batches, followed by analytical methods to determine the effects of the changes on the product.

The process could produce silica sols and gels with an ethanol concentration of or below 0.1 w-%. Dry weight determination was found to provide some information about the product but the method requires further improvement. Absorbance measurement was found to provide qualitative information about the effect of sol maturation on gelation time.

The method developed within this thesis can be used to produce acidic silica sols and gels of low ethanol concentration. While the process configuration is simple and somewhat suitable for the intended purpose, several aspects of the process and analytical methods demand further development in order to achieve sufficiently reproducible outcomes and reliable information.

KEYWORDS:

biomaterials, synthetic materials, silicon dioxide, ethanol, evaporation

OPINNÄYTETYÖ (AMK) | TIIVISTELMÄ
TURUN AMMATTIKORKEAKOULU

Biotekniikka ja Elintarviketekniikka | Biotekniikka

12.6.2012 | Sivumäärä 78

Ohjaaja: Mika Jokinen, Yliopettaja

Karlo Villa

ALHAISEN ETANOLIPITOISUUDEN SILIKASOOLEJA SOLUKAPSELOINTIIN

3D-solukapselointi on menetelmä jota käytetään solubiologian, kudosteknologian ja kemikaalien testauksen yhteydessä. Erilaisia materiaaleja on tarjolla solukapselointia varten. Biologista alkuperää olevien materiaalien etuna on biologinen yhteensopivuus mutta niiden laatu voi vaihdella. Synteettisillä materiaaleilla voidaan saavuttaa parempi toistettavuus mutta toiminnallisuuden edellytyksenä voi olla materiaalin muokkaaminen. Yksi luokka synteettisistä solukapselointimateriaaleista ovat synteettiset silikasoolit ja geelit.

Synteettisiä silikasooleja ja geelejä voidaan valmistaa piialkoksidien hapolla katalysoidun hydrolyysin ja silika-aggregaattien emäksellä katalysoidun kondensoitumisen kautta. Tetraetoksisilaanin (TEOS) tapauksessa reaktion sivutuote on etanoli, joka on haitallista joillekin solutyypeille ja siten sen poistaminen ennen materiaalin käyttöä solukapselointiin on tarpeellista. Opinnäytetyön tavoitteena oli kehittää prosessi alhaisen etanolipitoisuuden silikasoolien ja geelien tuottamiseen solukapselointitutkimusta varten.

Haihdutusprosessi kehitettiin etanolin poistamiseen happokatalyysin avulla tuotetuista silikasooleista ja geeleistä. Lisäksi kahta menetelmää, kuiva-ainemääritystä ja absorbanssimittausta, sovellettiin soolien ja geelien ominaisuuksien tutkimiseen. Etanolin pitoisuus silikasooleissa ja geeleissä määritettiin headspace-kaasukromatografialla. Prosessin kehitys totetutettiin muuttamalla prosessin kestoa eri tuotantoerien välillä ja analysoimalla muutosten vaikutus tuotteeseen.

Prosessilla voitiin tuottaa silikasooleja ja geelejä joiden etanolipitoisuus oli 0.1 m-% tai vähemmän. Kuiva-ainemäärityksen todettiin tarjoavan jonkin verran tietoa tuotteesta mutta menetelmä vaatii jatkokehitystä. Absorbanssimittauksella voitiin tuottaa laadullista tietoa soolin maturaation vaikutuksesta geelautumisaikaan.

Työssä kehitettyä menetelmää voidaan käyttää alhaisen etanolipitoisuuden silikasoolien ja geelien tuottamiseen. Siinä missä prosessin kokoonpano on yksinkertainen ja jossain määrin sopiva tarkoitukseensa nähden, useat prosessin ja analyysimenetelmien ominaisuudet edellyttävät jatkokehitystä riittävän toistettavien lopputulosten saavuttamiseksi ja luotettavan tiedon keräämiseksi.

ASIASANAT:

biomateriaalit, synteettiset materiaalit, piidioksidi, etanoli, haihdutus

CONTENT

APPENDICES

FIGURES

TABLES

LIST OF ABBREVIATIONS (OR) SYMBOLS

sol-gel	e.g. a process that features the transition from a sol to a gel
sol/gel	materials that are formed via a sol-gel transition
PVA	poly(vinyl alcohol)
PEG	poly(ethylene glycol)
PLGA	poly(lactic-co-glycolic acid)
TEOS	tetraethoxysilane or tetraethylorthosilicate
ECM	extracellular matrix
rBM	reconstituted basement membrane
EHS	Engelbreth-Holm-Swarm-tumor
GAG	glycosaminoglycan
HA	hyaluronic acid
IC50	50 % concentration where a compound inhibits biological or biochemical function
RGD	amino acid sequence Arginine-Glycine-Aspartic acid
MMP	matrix-metalloprotease
PEO	poly(ethylene oxide)
PAA	poly(acrylic acid)
PLA	poly(lactic acid)
TMOS	tetramethoxysilane or tetramethylorthosilicate
ORMOSIL	organically modified silane
Et	ethyl
Me	methyl

1 INTRODUCTION

Cells, especially those of higher organisms, are very sensitive to the conditions in their microenvironment. Immobilization in a suitable matrix can provide improved stability of cultured single cells when compared to traditional methods of long-term cultivation. (1) Immobilization of catalytic materials in artificial matrices has been shown to provide attractive alternatives to traditional suspension-based applications where a biocatalyst is dissolved or suspended in a solvent, *e.g.* enzymatic conversion of starch to sugars. A variety of materials of synthetic or biological origin are available for the encapsulation of biological materials and the variety of potential applications is considerable. (1)

The limitations of two-dimensional cell culture techniques in terms of *in vivo* comparability have been established (2) and reported examples of the greater *in vitro* accuracy of 3D models include testing of a cytotoxic compound for a breast cancer cell line (3) and organotypic cultures of pancreatic cancer cells (4). While the need for more relevant cell models and alternatives to animal models has been actualized in the cosmetics industry as a response to stricter legislation (5) and the 3R principle, the pharmaceutical industry is still waiting for more affordable and reliable high-throughput assays to come available (2). While high-throughput methods for cancer cell spheroid cultivation are available (6), the shift from established to new technologies will require time and resources. (7)

The benefits of synthetic matrices over matrices of biological origin are evident in the light of potential clinical applications of the matrices. Matrices of biological origin feature inter-batch variations in composition and quality. While this is tolerable in research, the desire for higher repeatability, more controlled conditions and strict quality requirements for clinical applications limits the use of established cell encapsulation matrices of biological origin. Synthetic organic materials solve the issue of batch-to-batch repeatability, but may suffer from issues like swelling or degradation over time. (2)

Silica is abundant in the lithosphere and widely spread in the biosphere. Several organisms use silica directly as a structural material in their bodies. Amorphous silica matrices for cell encapsulation are still mostly under research, and a variety of studies have studied the encapsulation of microbes and plant and animal cells in silica hydrogels. (1)

Silica hydrogels can be produced from aqueous colloidal silica solutions by a sol-gel process. A silica sol can be produced by acid or base catalyzed hydrolysis of alkoxysilanes. The process yields silicic acid and alcohol. Silicic acid can condensate into silicon dioxide particles in different conditions. When the condensation and aggregation of particles progresses far enough to produce a network of aggregates that envelopes the liquid phase, a gel is formed. (8) Silica gels are an attractive alternative to animal-based materials and synthetic materials because their can be modified by adjusting processing conditions.

The structural properties of sol-gel derived materials can be adjusted by changing the chemical composition of the sol precursor and the conditions during processing. Components with nutritional or other functionalities can be incorporated into the gel matrix easily by mixing them into the sol prior to gelation. (1) Sol/gel silica encapsulation processes have been reported, among others, with pancreatic islets (9), *E. coli* (10), cyanobacteria (11), fibroblasts, and epithelial cells (12).

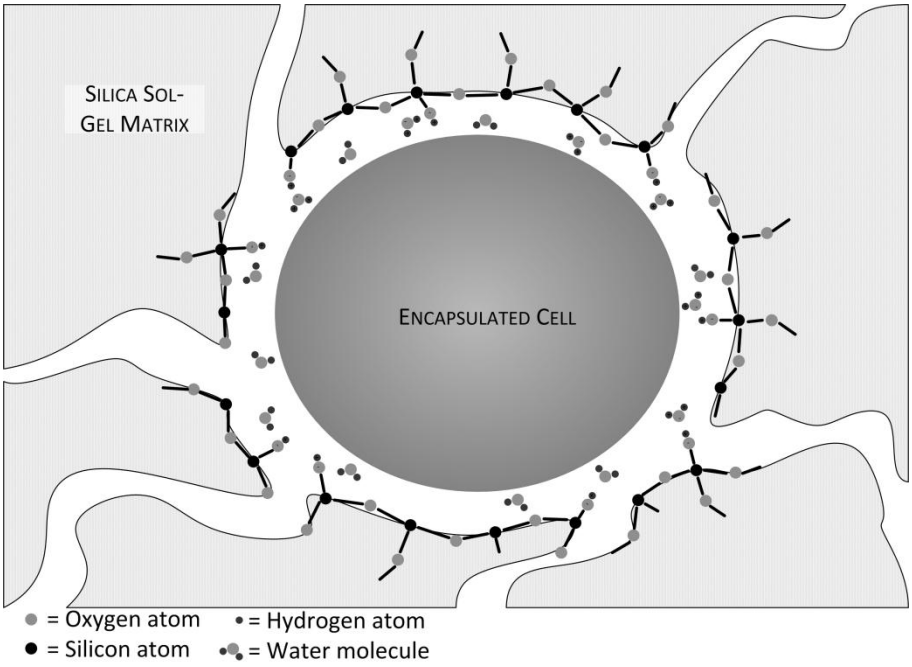

Figure 1: Principle of encapsulating cells in silica gels. The cell is surrounded by a layer of solvent encapsulated inside a silica sol/gel matrix. Pore structure allows for transport of nutrient and waste compounds. Reproduced with permission from Dickson, 2011 (11).

The use of alkoxide precursors, *e.g.* tetraethylorthosilicate (TEOS), and the subsequent generation of alcohol, *e.g.* ethanol, to over an 4 M concentration in reported sol preparations (12) is considered to be a significant limitation in the sol/gel encapsulation of biological materials. While evaporation methods have been applied to generate biocompatible routes for encapsulation (10) (12), ethanol concentrations as low as 20 mM have been shown to have a significant effect on human neuroblastoma proliferation (13) and concentrations of 50 and 100 mM can induce apoptosis in human epidermoids and mouse fibroblasts (14). Therefore it is relevant to consider alcohol removal when preparing alkoxy-derived silica sols for encapsulation of mammalian cells. While silica sols can be produced with ethanol as a solving agent (8) it is not necessary as the immiscible TEOS-water system still features hydrolysis at the phase boundary layer and phase dispergation can increase the available surface area significantly. In spite of this, TEOS is an attractive choice due to the low cost and the possibility to adjust gel structure and biodegradability by different processing methods.

Alcohol separation from water-alcohol systems via distillation is a common process in the chemical and food industries. With water-ethanol solutions containing colloidal silica particles boiling ethanol at normal atmospheric pressure poses risks of unwanted irreversible interactions between the silica particles (15).

Evaporation is a physical phenomenon which occurs at the liquid-gas phase boundary layer under a wide range of conditions. The rate at which evaporation occurs depends on the degree to which the equilibrium state is achieved in terms of liquid and gas phases.

Ethanol quantification is possible by enzymatic, physical or chromatographic methods. When considering the properties of silica sols and gels as materials subjected to analysis, capillary gas chromatography with headspace sampling is the most suitable method because of its sensitivity and wide range of detected analyte concentrations.

The gelation of sol/gel systems can be examined with different analytical methods. Within the scope of this study an improvised method was tested to estimate the gel time of a silica sol when mixed with cell culture media.

The aim of this thesis was to develop an evaporation process to supplement acidic pathway of silica sol production from TEOS. Specifically the aim was to determine process equipment and processing parameters for producing sols with a low ethanol content for cell encapsulation.

2 PREVIOUS WORK ON SILICA GELS

Research and development project titled “Cell-In-Gel” undertaken at Turku University of Applied Sciences, Turku, deals with research and development of silicon dioxide hydrogels for cell encapsulation applications.

This thesis is conducted as a part of that project.

The project hosted a pilot project integrating engineering studies in a R&D-project (16). Some of the work conducted within this pilot project is used as background information in this thesis. Short summaries of studies done under the project are presented in the following sections.

2.1 Enzyme encapsulation

A glucoamylase (EC 3.2.1.3. Sigma) was encapsulated in a TEOS-derived sol which was partially dried and preserved in moist condition. The embedded catalyst was packed into a chromatography column (Amersham Biosciences, XK26) that was used as a plug flow reactor operating in continuous mode. The hydrolytic performance of the embedded enzyme was compared to a batch process in a stirred tank bioreactor (CelliGen, New Brunswick Scientific Co. Inc.) in terms of starch conversion to glucose.

The catalytic performance of the enzyme was preserved in spite of exposure to potentially high ethanol concentrations during the encapsulation. The performance of the plug flow reactor, estimated by the change in concentration of glucose in the outflow, was considerably lower than that of the batch process. Poor performance was not unexpected when considering that the encapsulation process was conducted for the first time and not optimized in any way for maintaining activity of the enzyme.

2.2 Process development

Sol production process was scaled up from <50 mL to <500 mL scale by adapting a bioreactor (Biostat B2. B. Braun Biotech International GmbH) for an

aseptic production process with pH adjustment between 2 and 7 and temperature adjustment from room temperature to approximately 10°C and below. The asepticity of the process was preliminarily shown by microbiological methods.

The system was found to be suitable for producing sols with variable R-values. While temperature control by the control unit alone was considered insufficient in terms of range and reliability, adding external circulation showed potential for steadier temperature adjustment.

An improvised temperature control system mimicking the water jacket principle of a bioreactor was assembled for evaporation experiments in a smaller scale of 30-100 mL. With the improvised system a steady and repeatable temperature profile was achieved and the range of control was established for 5-60°C.

The requirement of determining ethanol concentration in the sol after evaporation was addressed by reviewing available analytical methods for ethanol quantification. Full evaporation headspace gas chromatography method with flame ionization detector (FE-HS-GC-FID) was adapted from literature (17).

Alcohol evaporation was conducted by holding the sol at 60°C for 70-110 minutes. The R-value, meaning the molar ratio of water to TEOS, varied between 5 and 200 and the batch size between 30-100 mL. Change in ethanol concentration was determined by gas chromatography methods described in Chapter 6. The result was that in the described time frame it was possible to achieve, on average, 73 % reduction from initial ethanol concentration. However, the reproducibility and predictability of the process were not at a satisfactory level due to limitations in the process equipment.

This thesis contains the work that followed, meaning the further scaling of process equipment to adjust for measurement inaccuracy and the optimization of evaporation process duration for producing low-ethanol silica sols for cell encapsulation.

3 USE OF 3D CELL ENCAPSULATION

Cells are responsive to the variations in their environment (18). Cells from higher organisms such as mammals are more sensitive to environmental variations than micro-organisms. *In vivo* mammalian cells are mainly attached to other cells and/or an extracellular matrix (ECM) which is formed by combination of proteins and proteoglycans (19). Gene expression is guided partially by the signals and cues in the environment. The differences in cell behavior between 2D and 3D culture methods can be considerable. For example, comparison of epithelial cells cultured in 2D and 3D systems suggest that a three dimensional environment allows for longer proliferation time. (20)

This chapter presents examples of fields of application and methods for cell encapsulation. Commercially available materials and methods and previously reported use of sol-gel derived silica are briefly reviewed.

3.1 Basic cell research

Cell biology research could benefit from 3D structures resulting in increased *in vivo* resemblance of cellular behavior. Functional properties like oxygen and nutrient delivery or waste disposal, mechanical support, application of physical stimuli accompanied with consistent quality and the possibility to apply established analytical methods like immunostaining and microscopy are all expected from new materials. (21)

3.2 Tissue engineering

Previously mentioned features of cellular behavior in 3D microenvironments are also appreciated in generation of artificial tissues and in clinical therapies that apply living cells *in situ* to act as producers of therapeutics or to act as precursors for new tissue or guiding tissue regeneration. (22)

3.3 Testing of chemicals

European Union's regulation about chemical legislation, REACH, mandates more extensive knowledge about potential toxicity of chemicals. Some *in vitro* skin corrosion tests using artificial skin have already been accepted for chemical testing. However, the condition for accepting data from *in vitro* models is that they are validated and appropriate for their intended use. (5) In other words, new models are expected to replace, reduce or refine the use of animal testing - if these conditions are not met, a new model is not likely to gain approval.

3.4 Established 3D cell culture materials

A variety of materials and methods are available for 3D cell culture. A list from drug development perspective is provided by (2). Those that are based on formation of a hydrogel, *i.e.* a multi-phase system where the primary phase is liquid water, are presented in Table 3.1. Animal-based and functionalized synthetic materials may have very different effects on cell behavior, such as migration, depending on their often variable and dynamic physical properties such as stiffness, pore size and small-scale deformability. (23)

Table 3.1: Commercially available hydrogels for 3D cell culture. According to Rimann & Graf-Hausner, 2012 (2).

Brand	Vendor	Material	Biodegradable	Animal components
Extracel	Glycosan Biosystems	Hyaluronane, Gelatine, PEG	Yes	Yes
AlgiMatrix	Invitrogen	Alginate	Yes	Yes
QGel	QGel	PEG	Yes/No	No
PureCol	Advanced BioMatrix	Collagen 1	Yes	Yes
BD Matrigel	BD Biosciences	Basement membrane	Yes	Yes
3D Life PVA Hydrogel	Cellendes	PVA, PEG	Yes	No
PuraMatrix	3DM Inc.	Synthetic oligopeptide	Yes	No

Spheroid-shaped cancer cell aggregates are used as 3D models for studying cell physiology and responsiveness to therapeutic agents. While spheroids lack some properties of actual tumors, they are considered to be improved models when compared to monolayer cell cultures. (24) A general trend in spheroid generation is research into automated and reliable methods for HTS purposes.

A rapid method for generating spheroids in U- or V-bottom 96-well plates with centrifugation is described in (24). However, compared to the hanging drop method centrifugation involves momentarily high shear rates that may reduce cell viability. Additionally the method may require addition of animal-derived basement membrane preparations (*e.g.* Matrigel) to induce cell aggregation. (24) While the exact method of operation of supplements is not fully understood, aggregation may be caused by a combined effect from modification of the physical properties of the cellular environment and chemical cues from the supplement.

Vendors who provide readily grown organotypic spheroids or methods for generating spheroids for drug candidate testing are presented in Table 3.2. Spheroid generation in a hanging drop is claimed to enable heterogeneous cell culture and high throughput operation but requires automation to remain reasonable in terms of workload.

Table 3.2: Organotypic spheroids for 3D cell research, commercialized and general methods. According to Rimann & Graf-Hausner, 2012 (2).

Brand	Vendor	Method	Format
Microtissues	InSphero AG	Hanging drop	96-384 well plate
NanoCulture Plate	Scivax	µ-textured surface	96 well plate
Perfecta 3D Plate	3D Biomatrix	Hanging drop	384 well plate
U/V-bottom plates	Several	Centrifugation	96 well plate

Seeding cells into a 3D scaffold is not used only in research or cell culturing but also potentially in tissue engineering for introducing living hybrid materials *in situ* (1). While large polymer matrices increase the surface area available for cell attachment, the situation may not differ significantly from a 2D dimensional monolayer if the cells are spread on the curved surface of a polymer fiber with a diameter of *e.g.* 300 µm. Out of the materials presented in Table 3.3 Alvetex is the only one that features primarily void bulk pore volume and 5-20 µm pore size that actually results in 3D environment.

Table 3.3: Synthetic scaffold materials for 3D cell culture. According to Riemann & Graf-Hausner, 2012 (2).

Brand	Vendor	Material	Degradable	Structure
Alvetex	Reinnervate	Polystyrene	No	Sponge
3D-Insert PLC	3D Biotek	Polycaprolactone	Yes	Fiber array
3D-Insert PS	3D Biotek	Polystyrene	No	Fiber array
3D-Insert PLGA	3D Biotek	PLGA	Yes	Fiber array

In addition to porous and rigid scaffolds or elastic hydrogels so-called microfluidic arrays have become available for culturing embedded cells. These utilize passive transport of fluid driven by gravity and/or capillary forces to create an infusion culture. In principle the benefits of these devices include improved nutrient cycle, smaller requirements for cells and encapsulation matrix, reduced workload and compatibility with automation via liquid handling robotics and imaging methods via clear plastic materials. (2)

3.4.1 Hydrogels

From the point of view of cell encapsulation hydrogels often consist of relatively small volume-fraction of cross-linked polymer matrix that incorporates the cells and bulk fluid. The fluid is typically a nutrient medium. It is crucial that the porosity of the gel does not significantly inhibit diffusion of nutrients, gases or waste products while preventing leakage of cells. (25) In addition to supporting cell behavior, the mechanical performance of the gel in *in vitro* and *in vivo* conditions is considered to be a significant factor (26). The physical, biological and chemical properties of the gel have a complex and important effect on the proliferation of encapsulated cells. However, properties of bulk material may not represent the microenvironment that the cells are in contact with, *i.e.* substrate stiffness may not be directly measurable with tensile or compressive tests. (27)

3.4.1.1 Non-synthetic

Non-synthetic encapsulation matrices include materials that have similar properties with or originate from the ECM. This chapter presents some examples of existing non-synthetic cell encapsulation matrices researched and applied in cell biology and tissue engineering.

Collagen is the most abundant protein in animal tissues and therefore it is considered to have great potential for applications where enzymatic hydrolysis by metalloproteases is not an issue, but may even be purposeful in terms of allowing cells to invade the matrix. (25) While synthetic self-assembling collagen hydrogels have been described by O'Leary *et al* (28), commercially

available and most widely used collagen products, *e.g.* collagen 1 preparations, are derived from animal sources like rats or bovines.

Reconstituted basement membrane (rBM) from murine Engelbreth-Holm-Swarm-tumor (EHS) has been used to produce a hydrogel with significantly higher biological activity in terms of cellular differentiation and proliferation than collagen hydrogels alone (29). rBM from EHS-tumor is available under commercial labels (Matrigel, Cultrex) and protocol for preparing rBM is provided in literature (30). Matrigel has been used to generate protocols for angiogenesis assays with different cell types. In spite of this and other extensive use spanning more than two decades complete understanding of the functionality is still missing. (31)

Products from animal sources feature properties that are undesirable from the perspective of developing validated models for drug development, *i.e.* batch-to-batch variations in product properties and quality. Additionally, tissue engineering applications require that the matrices cause a very low or no immune response at all. (25) The interference of matrix components with analytical methods is an additional drawback. For example, autofluorescent properties of collagenous material sets limitations for the use of diagnostic tools. (2)

Hyaluronic acid (HA) is endogenous glycosaminolglycan (GAG) for mammalian tissues and it has been utilized to produce cross-linked hydrogels with good biocompatibility and biological activity. It is readily degradable by cells and can be modified to acquire different properties depending on the application. (25) For example, cancer cells exhibited a more biomimetic response to antimitotic drugs when embedded in a HA hydrogel, *i.e.* the *IC50* concentration for hydrogel encapsulated cells was higher when compared to a monolayer culture (32). HA-based hydrogels have been commercialized by Glycosan Biosystems, Inc. under HyStem and Extracel -labels. The HA is produced via *Bacillus subtilis* fermentation. While HyStem is supplemented with PEG-diacrylate (33), Extracel is supplemented with gelatin from bovine sources and heparin from porcine sources (34).

Alginate and chitosan are both linear polysaccharides derived from biological sources: seaweed or bacteria and arthropod exoskeletons, respectively. Both feature biocompatibility, biodegradability and gelation when introduced to physiological conditions like presence of Ca^{2+} or physiological pH. Several modifications for customization in terms of pore structure, mechanical properties and gelation exist. While alginate beads have been utilized in medical applications, it presents low toxicity and variation in isolate composition. Some methods for inducing gelation in chitosan, *e.g.* UV irradiation, may not be suitable for *in vitro* encapsulation of cells. (25)

Non-synthetic encapsulation matrices often provide good biological response, support biomimetic cellular behavior and their properties can be modified to some extent. However, the sources and complex compositions of materials may pose challenges for repeatability and validation of assays or applications.

3.4.1.2 Synthetic

Synthetic hydrogels do not differ from non-synthetic materials in their principle of operation, *i.e.* they provide a 3D microenvironment to promote cell proliferation. However their composition and properties are much more accurately defined and modifiable by chemical methods. This chapter presents some examples of available synthetic hydrogels for cell encapsulation.

Polyethylene glycol (PEG) is a commonly used material because it can be modified with great variability. It is also biocompatible and chemically synthesizable. While PEG alone is biologically inert, *e.g.* cells do not recognize or attach to it, it is possible to functionalize the side chains with peptide sequences and enzymatically hydrolysable cross-linking bonds. This results in a completely synthetic material with adjustable biophysical and degradation properties. (35) Multi-armed PEG with matrix-metalloproteinase (MMP) - degradable or stable cross-linkers and cell-adhesion motif amino acid sequence arginine-glycine-aspartic acid (RGD) have been commercialized by QGel SA under the QGel-label.

Some other polymeric materials with small molecular weight monomers include poly(ethylene oxide) (PEO), poly(vinyl alcohol) (PVA), poly(acrylic acid) (PAA). Hydrogels can be prepared by cross-linking monomers with UV-exposure in the presence of a photoinitiator or with repeated freeze-thaw cycles in aqueous solutions containing a cross-linking agent (25). While these methods do not allow for biocompatible encapsulation of cells by forming the gel around them, the possibility of lyophilizing and reconstituting or thermally reversing the hydrogel between synthesis and application addresses the problem. While some polymers (*e.g.* poly(lactic acid) (PLA)) are biodegradable by default, synthesizing copolymers with varying ratios of hydrolytically degradable and undegradable subunits allows for greater control over material properties (25).

Reversibly self-assembling peptides capable of forming hydrogels were initially produced via recombinant DNA technology (36). Synthetic oligopeptides are the a natural way to mimic the extracellular environment in terms of physical and chemical structure (37). Research of RAD16-I based hydrogels has resulted in commercialized product by 3DM Inc. under the label PuraMatrix. This material is shown to have a primary sequence (RADA4) that promotes cell adhesion (38) and self-assembles into β-sheet-secondary structures in order to form nanofibers (39). The material, which has similar *in vitro* performance as Matrigel, can be functionalized with motifs for cell adhesion, migration and differentiation (40).

Synthetic materials offer greater modifiability and higher quality over non-synthetic materials. However they may not feature biomechanical properties required to provide an environment similar to non-synthetic materials. Additionally characteristics like swelling, degradability, protein absorbance, possibility of cell recovery and compatibility with analysis methods need to be considered when reviewing different materials.

3.5 Sol-Gel derived silica as encapsulation matrix

Sol-gel derived silica has been used for a large variety of applications ranging from optical to electronic devices, separation technologies, adsorption and

biosensing (11). While first applications with biological compounds were experimented already more than half a century ago with enzymes, further progress has occurred mostly in the post 1990-era (1). First examples of living cells that encapsulated in sol-gel derived silica gel from TEOS-precursor were *Saccharomyces cerevisiae* in 1989 (41). The choice of organism was partly affected by its resistance to ethanol that is a product of precursor hydrolysis reaction (1). Cells entrapped with the same method were used as biocatalysts for sucrose degradation in a similar study a few years later (42).

Sol/gel encapsulation of mammalian cells (murine pancreatic islets) with clinical application perspective (*in situ* insulin production) was reported in 1998 (9). Further clinical applications were studied in the form of an artificial liver where hepatocytes were encapsulated within a hybrid collagen-silica matrix. Already in this report the process was described as biocompatible due to low concentrations of ethanol present in the gas-phase driven formation of a gelatineous coating. However, the method does not utilize silica only as a hydrogel but rather as a mechanical support for a softer hydrogel that contains the cells. In addition the method utilizes a variety of precursors in addition to TEOS to achieve desired properties for the material. (43)

More recently the biocompatible use of TEOS-derived silica gels have been demonstrated with fibroblasts and epithelial cells. Viability of the cells was enhanced by adding glucose to the sol as a porogen and a nutrient, and by adjusting the trypsinization to achieve clumps of cells. While morphological characteristics of encapsulated cells differed from adherent cells and proliferation or spreading was not detected, viability determination after encapsulation suggests that the cells survive the process. (12)

4 SOL-GEL PROCESSING OF SILICA

Sol-gel processing is a general way to refer to materials processing that involves two distinct steps, here described for silica: 1. generation of a suspension of colloidal silica particles, a sol; 2. condensation and aggregation of said particles into larger aggregates and further into a network that envelopes the entire volume of the original suspension, a gel. (8)

The sol consists of small particles suspended in solvent phase. The particles in a colloidal solution are so small (1-100 nm) that they are only affected by short distance interactions like van der Waals forces and surface attractions while their movement is based on Brownian motion. While the particles are not part of any polymeric structure they are considered to form a particulate sol. Even when monomeric silica, more accurately silicic acid ($Si(OH)_4$), particles form di/oligo-to-polymeric structures that condense or accumulate together and further form aggregates, the particle size is at first only at the border on being considered colloidal, *i.e.* 1 nm. (8)

The formation of a gel requires that the aggregates form a network that extends the entire geometry of the liquid phase. While the entire system is still formed of two phases, they are both now of colloidal dimensions in terms of porosity. (8)

4.1 Precursors

Two examples of a silicon atom with alkoxy ligands, tetraethoxy- and tetramethoxysilane (abbreviated TEOS and TMOS), are often used to produce silica sols and gels. These silicon alkoxides, or alkoxysilanes, consist of a central silicon atom with four alkyl ligands joined to the center via an ester bond. A simplified structural formula of an tetraalkoxysilane is presented in Figure 2.

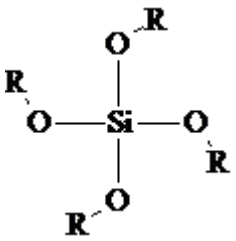

Figure 2: Generic alkoxysilane. -R represents an alkyl (Me/Et) group.

In addition to alkoxy groups the ligands can be alkyl groups, meaning that there is no ester bond between the ligand and the central atom. Compounds where one of four alkoxy ligands is replaced with a methyl, ethyl or a larger alkyl group are called organically modified siloxanes, abbreviated as ORMOSILs. Because the Si-C-bond is more stable than Si-O-C -bond, their properties depend on the size of the organic ligand, *i.e.* a significantly longer alkyl ligand produces different steric effects when compared to Me/Et ligands. (11) Because of substantially higher reactivity of alkoxy-ligands they are referred to as functional groups, *i.e.* tetraalkoxysilanes are considered tetrafunctional while an organotrialkoxysilane or a diorganodialkoxysilane would be tri- of difunctional, respectively.

Along with the possibility to substitute an alkoxy ligand with an alkyl ligand comes the opportunity of further modifying the ligand to gain functional properties. (11)

The only precursor used in this thesis was tetraethoxysilane.

4.2 Hydrolysis and condensation

Alkoxysilanes readily react with water when the alkoxy group (OR) is detached from the silicon and replaced with an hydroxyl group (OH):

$$\equiv Si - O - R + H_2O \leftrightharpoons \equiv Si - OH + ROH \quad \text{Eq. 4.1}$$

The forward exothermic reaction, hydrolysis, occurs in tandem with the reverse reaction, esterification. Under suitable reaction conditions hydrolysis may complete fully so that all OR groups are replaced:

$$Si(OR)_4 + 4H_2O \longrightarrow Si(OH)_4 + 4ROH \quad \text{Eq. 4.2}$$

The problem with using alkoxides in biological applications becomes apparent here - at minimal theoretical molar ratio *R* for water:precursor of 4[1] resulting sol would stoichiometrically consist of only silicic acid and alcohol, even though in reality water is released from condensation reactions following hydrolysis. Even at relatively high *R*-values the resulting alcohol concentration is high from biological point of view, *e.g.* at water:TEOS -ratio of 50 the resulting sol would contain almost 21 v-% ethanol.

Hydrolysis occurs even at acidic conditions to the extent that esterification becomes negligible in terms of total reaction progress. Hydrolysis of TEOS occurs when the ethoxy ligand is replaced by a hydroxyl group from water. With excess water the rate of hydrolysis is increased and full hydrolysis can be expected, *e.g.* at R-value of 10 in acid catalyzed conditions unhydrolyzed precursors (Q_0(0.4) -species, *i.e*. at least one ligand is hydrolyzed)[2] are no longer present after one hour and only Q_0(4.0) and Q_0(3.1) remain after two hours. (8) Hydrolysis is considered proceed to full completion in a high-R-reaction relatively fast (8), which is desirable from viewpoint of biological applications as hydrolysis of TEOS after introducing a biological component may result in toxic effects caused by released alcohol (11).

[1] The complete reaction from precursor to fully condensed gel can be expressed as $Si(ROH)_4 + 2H_2O \longrightarrow SiO_2 + 4ROH$, hence the lowest theoretical R-value for entire sol-gel process would be 2.

[2] Nomenclature for distinguishing different stages of hydrolyzed precursors follows Q_0(x,y)-form where x and y reflect monomer composition in $Si(OH)_x(OEt)_y$. (8)

Hydrolysis can be catalyzed by acids or bases, mineral acid HCl being the method used in this work. Catalytic effect is based on lowering the pH near or below 2 which is the isoelectric point for silicic acid. Catalytic effect is observed at dilute concentrations (pH≤5) but duration of hydrolysis in lower concentrations may take thousands of hours. (8) (11)

When water is the only solvent present in the beginning of hydrolysis, the reaction is accelerated by the formation of ethanol and subsequent reduction of phase separation (8). Additionally some acceleration could be attributed to increase in temperature of the reacting mixture as hydrolysis releases energy. However this effect can be expected to have very little effect in high R-value reactions where bulk water absorbs the released energy.

Condensation can occur in the form of alcohol condensation where an unhydrolyzed alkyl group reacts with a hydroxyl group from a hydrolyzed ligand.

$$\equiv Si - OR + HO - Si \equiv \leftrightharpoons \equiv Si - O - Si \equiv + ROH \qquad \text{Eq. 4.3}$$

Alcohol condensation requires that a sol contains precursors that are not fully hydrolyzed. As mentioned before, this is an unfavorable reaction when occurring during the encapsulation process as alcohol that is released is potentially harmful for biological components.

Water condensation occurs similarly to alcohol condensation but the reaction product is, in case of monomer silicic acid reactants, silicic acid dimer and water:

$$\equiv Si - OH + HO - Si \equiv \leftrightharpoons \equiv Si - O - Si \equiv + H_2O \qquad \text{Eq. 4.4}$$

Because of water condensation the net reaction for preparing a TEOS-based anhydrous silica can be expressed as:

$$Si(OEt)_4 + 2\,H_2O \leftrightharpoons SiO_2 + 4\,EtOH \qquad \text{Eq. 4.5}$$

Condensation in a hydrolyzed acidic sol is partially inhibited by complete deprotonation of silicic acid in low pH. Additionally, the reaction balance in high R-value sol would favor hydrolysis which is the reverse reaction in Eq. 4.4.

4.3 Condensation

An acidic sol is only metastable, *i.e.* sol-gel transition occurs in spite of low pH, even if over a long period of time. The difference in gelation time between pH 3 and 2 can be over 3-fold[3].

Between pH 2-7 polymerization, or condensation, of silicic acid monomers as presented in Eq. 4.4 is considered to occur through two steps: first a deprotonated silanol is produced via proton capture by a hydroxyl ion (Eq. 4.6) which is followed by formation of and oxygen bridge between two silanols (Eq. 4.7). Gelation speed is considered to be proportional to $[OH^-]$. (8)

In a more practical scenario the presence of salts and other molecules, originating from cell culture medium, that interact with particle surface charges or affect the availability of water in the system also have an effect on the rate of condensation

$$\equiv Si - OH + OH^- \leftrightharpoons \equiv Si - O^- + H_2O \quad \text{Eq. 4.6}$$

$$Si - O^- + HO - Si \equiv \leftrightharpoons \equiv Si - O - Si \equiv + OH^- \quad \text{Eq. 4.7}$$

Dimers react with monomers to form linear trimers and subsequently tetramers. Formation of cyclic trimers is not favored at low pH but tetramers and larger cycles may form due to availability of chain ends in small linear molecules. (8)

At low pH the size limit for particles is 2-4 nm. Stabilization of particle size is result of Ostwald ripening[4] and it is caused by dissolution of smaller particles and growth of larger particles to a size limit depending on solubility of silica according to pH and temperature. At basic pH the particles grow to a larger size and eventually form a stable colloidal sol. The growth occurs via Ostwald ripening (see Figure 8) but involves the addition of monomers to larger particles instead of oligomer fusion. (8)

[3] For an R-4 sol at pH 2 ~90 hrs and at pH 3 ~20-30 hrs (8).
[4] Small particles experience higher solubility because of high surface curvature whereas larger particles experience lower solubility because of lower surface curvature.

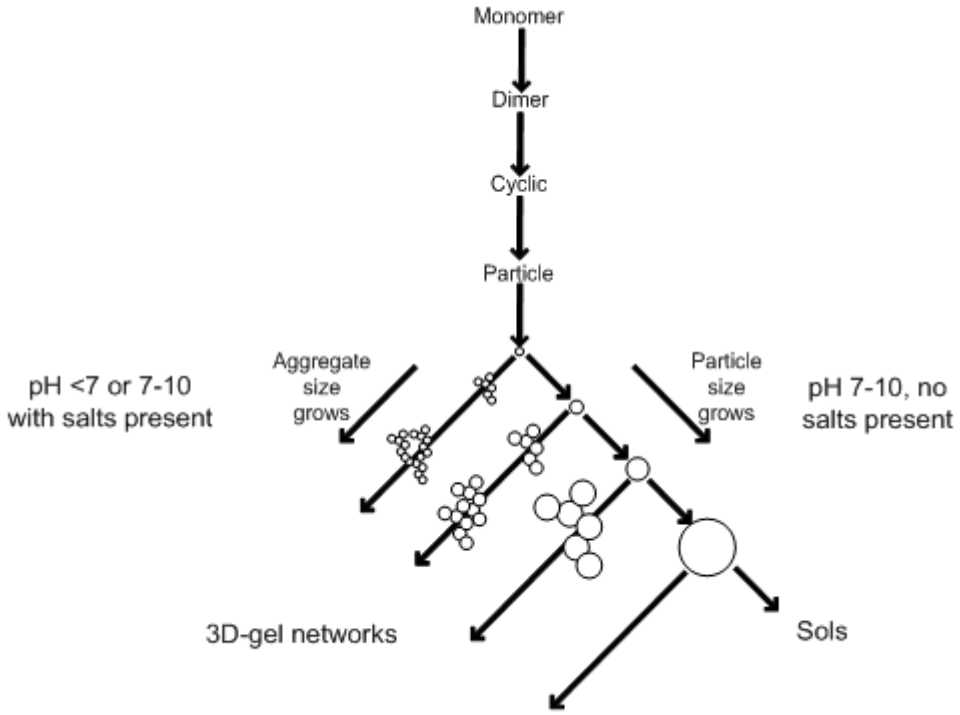

Figure 3: Polymerization behavior of aqueous silica. The process featured in this thesis reflects situations where pH is either 2 without salts and 7 with salts present, *i.e.* left hand side route. However, several intermediates are likely to coexist. According to Brinker & Scherer, 1990 (8).

Understanding of metastability of acidic sols is relevant for this thesis as the materials produced in the process are further used to study properties of gels. Additionally some of the materials are provided to partner institutions to be used in their corresponding studies.

4.3.1 Base catalyzed condensation

Condensation is fastest at pH 7 as here concentrations of protonated and deprotonated groups become similar, allowing reactions in Eq. 4.6 and Eq. 4.7 to proceed. (8) Relatively high speed of the reaction is beneficial as one desirable goal in encapsulation of mammalian cells is to prevent sedimentation of cells in pre-gelated mixture. However too high a speed may result in challenges in handling the sol/gel. It should be noted that while condensation occurs during the encapsulation process, aggregation becomes more significant as the degree of maturation increases. This claim is based on the concept that an acidic sol is metastable in terms of aggregate condensation. Whereas

primary particle size is presumed to remain within a narrow range of distribution, the number of aggregated particles grows as the sol matures.

Primary particles can form aggregates through random collisions with each other. An aggregate grows in size in a manner that depends on the mixture conditions. The density and porosity of the resulting gel depend on aggregate type. Pore size is a crucial factor for determining diffusion properties of small molecules within the gel.

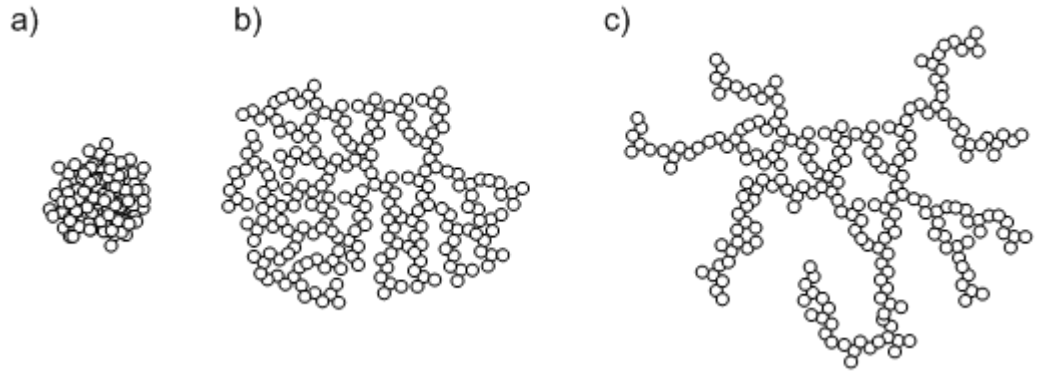

Figure 4: Equal weight aggregates that reflect the Eden growth model of fractals in neutral pH. a) A porous cluster which is not considered a fractal structure. Growth occurs only at the perimeter of the structure. b) Surface fractal. Growth occurs at the perimeter of the aggregate if porosity of the structure allows it. c) Mass fractal. Growth may occur as branching or extension of brances. Additionally, existing branches may join together in development towards a surface fractal. According to Brinker & Scherer, 1990 (8).

4.4 Gelation

Gelation occurs when clusters of condensed particles collide and combine to form a spanning cluster that extends to the full geometry of the liquid phase. Structurally the spanning cluster is a random, infinite molecule. At gel point viscosity of the fluid rises, *i.e.* more work is required to produce flow, and the material exhibits an elastic response to stress, *i.e.* the material returns to its original shape to some extent when stress is no longer applied. A simple definition is that when the sol does not pour upon tipping of the vessel gelation has occurred. However, at the point of gelation there exists several clusters that are not yet part of the spanning cluster but may be entangled in the structure.

Thus the system does not enter a static state but continues to experience hydrolysis and condensation. This is referred to as aging. (8)

Gelation time, often referred to as t_{gel}, is defined usually in terms of dynamic viscosity (η, dimension Pa.s) with a certain value which depends on the system under examination. Figure 5 demonstrates the principle of change in viscosity and elasticity of a material undergoing gelation.

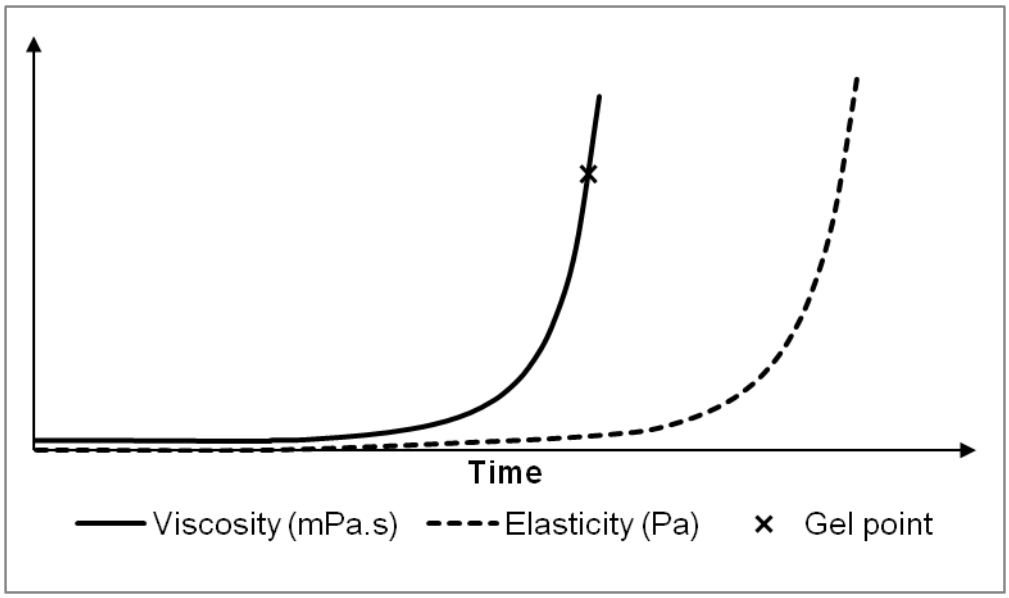

Figure 5: Example of evolution of viscosity and elasticity as a function of time for a silica sol/gel. Time scale here is arbitrary but may be anything from seconds to days. Additionally the lag between increases of viscosity and elasticity differs depending on the system. According to Brinker & Scherer, 1990 (8).

More accurate way of defining t_{gel} is to study the emergence of viscoelasticity in the sol/gel system. This is done by measuring shear stress τ (SS, defined as F/A, dimension Pa) as a function of shear rate $\dot{\gamma}$ (SR, defined as velocity/height, dimension s^{-1}) with a narrow gap viscometer that measures the phase delay of oscillations as they traverse through the fluid. When phase lag occurs the material exhibits viscoelastic behavior. Even as phase lag is observed, the gel undergoes flow. As gelation progresses further and the gel structure develops towards a spanning cluster, flow properties are eventually lost. Viscoelastic properties of gels are described more specifically by the components of complex shear modulus *G,* loss modulus *G''* and storage modulus *G'*, when observed at different oscillation frequencies ω. *G'* describes elastic properties

while *G''* describes the viscous properties of the sol/gel. The emergence of gel properties can be observed from either *G'* or *G''* or from *G* which is defined as *G=G'+iG''*. The evolution of *G'* and *G''* at fixed ω and as a function of the extent of reaction *p* are demonstrated in Figure 6.

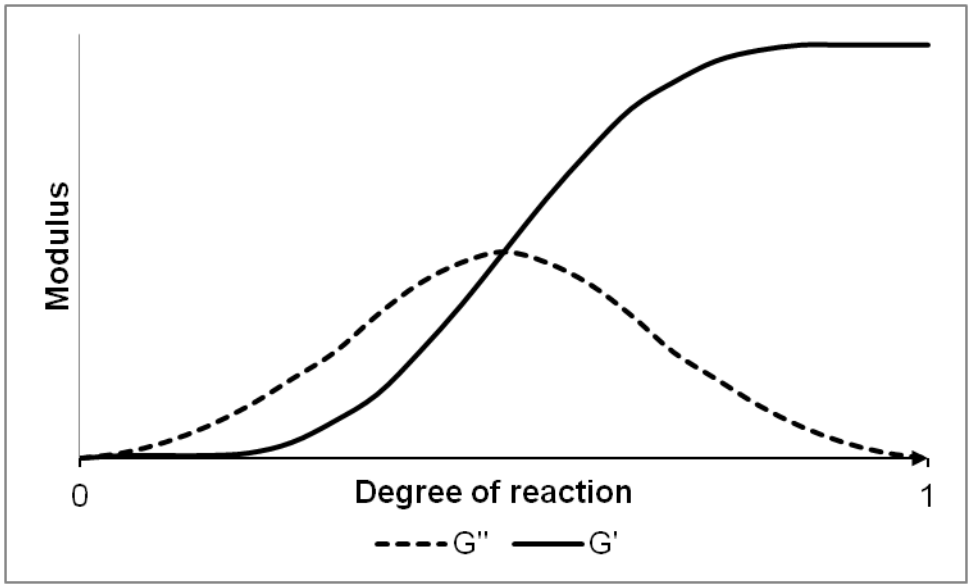

Figure 6: The evolution of loss and storage moduli *G''* and *G'* as a function of the degree of reaction. The illustration could be based on measurement data obtained with an oscillating rheometer operating at a fixed oscillation frequency ω. According to Brinker & Scherer, 1990 (8).

Initially evolution of the sol towards gel point was meant to be studied in this thesis by conducting measurements with a rotational viscometer. However, the intended instrument was not in operational condition and measurements were conducted for only a few samples. In any case the rotational viscometer is less than ideal for studying elastic samples as the rotation of the spindle would likely result in shredding of the gel structure. The principle of detecting gelation by rheological measurements is presented in Figure 7.

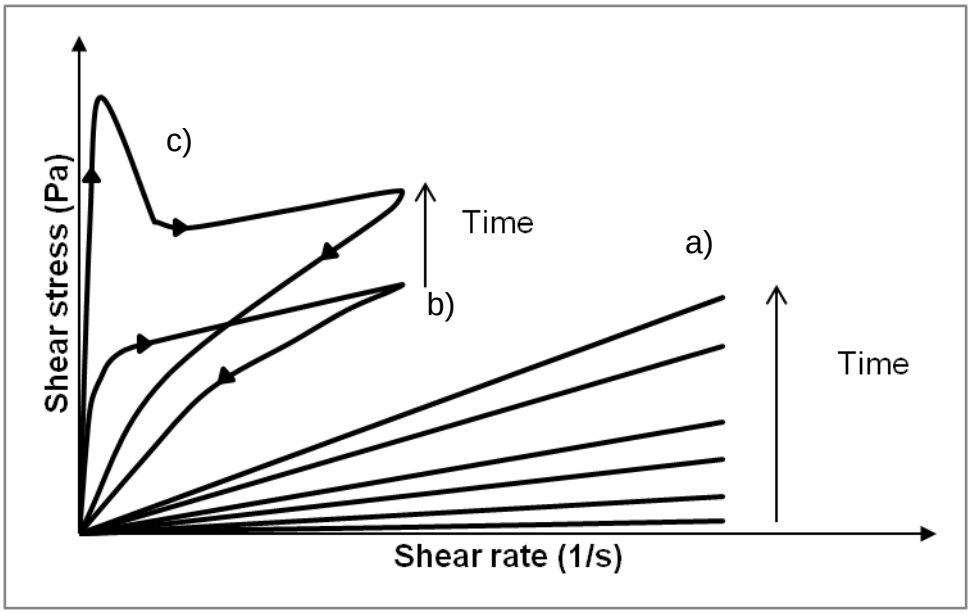

Figure 7: Shear stress as the function of shear rate at several time points. a) SS is directly proportional to SR and sol exhibits Newtonian behavior and viscosity increases as condensation progresses. b) Larger clusters are broken when shear rate increases. Sol exhibits shear thinning behavior. c) Gel exhibits load supporting or elastic behavior until yield stress is reached and the structure gives away. According to Brinker & Scherer, 1990 (8).

Observing the development viscoelastic properties of sols and gels in terms of cell encapsulation applications is related to the fact that cells or cell aggregates can sediment under gravity if the medium that they are in, *i.e.* neutralized silica sol/gel, is left to stand still. Thus knowing the time frame and understanding when a sol/gel is flowing, yet allows to maintain cells or cell aggregates in a state of suspension is important.

4.5 Aging of gels

Gelation presents a significant change in the physical properties of the sol/gel system. However, chemically the change is not as drastic. Time period after gelation that exhibits hydrolysis and condensation in the gel matrix is called aging. During aging some clusters may break apart or condense further while those clusters that were not a part of the spanning cluster at gel point will likely condense as parts of the spanning cluster. The structure of the gel may also undergo shrinkage, as is usually the case when gels are allowed to dry. While shrinkage is observed in wet gels as well, the extent to which the geometry of the gel changes is smaller. The relevance of shrinkage is

During aging aggregated particles experience coarsening. This is the result of different solubilities at different geometries of the particles. At regions of positive curvature the solubility is higher (as in the case of Oswald ripening) whereas in regions of negative curvature the solubility is lower. Coarsening is in effect dissolution and deposition of silica from the surface of a particle to the space between particles. This is called necking. The mechanism is illustrated in Figure 8. Coarsening results in stiffening of the gel structure. As solubility of silicates is higher in neutral pH, rate of coarsening is also higher in these conditions. Reaching equilibrium state depends on the temperature and pH. (8)

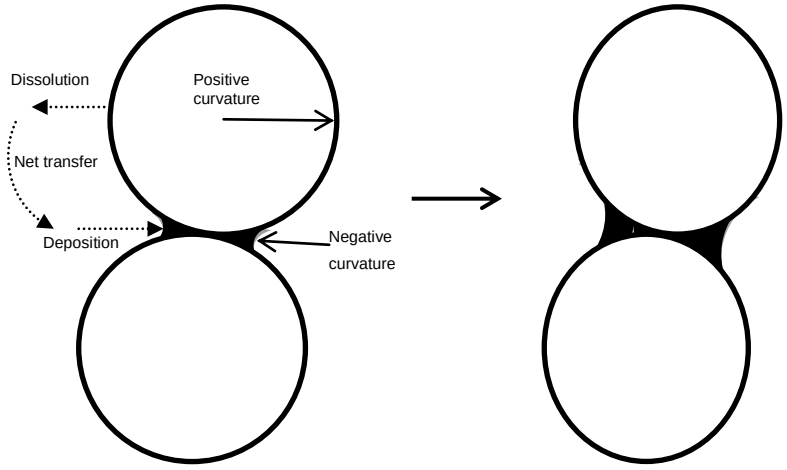

Figure 8: Coarsening or necking of aggregated particles. According to Brinker & Scherer, 1990 (8).

During this thesis an improvised procedure was implemented to observe the progress of maturation of silica sols and gels. The procedure was based on an observation that acidic and neutralized sols and gels obtained a cloudy appearance as gelation occurred during storage in a refrigerator or on the bench. The principle was to measure this decrease in transmittance of light with a spectrophotometer over a short period of time and to repeat the measurement over the course of several weeks. Changes in the sol/gel could then be observed from the measurement data.

4.6 Challenges associated with silica sols

Alkoxide derived silica sols and gels feature properties that should be considered when evaluating their usability in any application. Briefly, these include the release of alcohol during processing, potential toxic effects of nanoparticles and the dynamic nature of the sol/gel, system which poses challenges from a users perspective.

4.6.1 Alcohol

Ethanol released in hydrolysis (Eq. 4.2) presents problems with cytotoxicity and reduced viability during encapsulation. Published literature (10) (12) describes application of evaporation methods to reduce alcohol concentration in TMOS/TEOS derived silica sols prior to encapsulating living cells.

While some organisms are able to use methanol as an energy source (44) and moderate concentrations of ethanol in the growth environment are not detrimental for fermenting yeasts, this is not the case for most living organisms. From a tissue engineering perspective even small concentrations (20-100 mM) can be harmful to cells and tissues in a variety of ways (13) (14) (45). While cited experiments were performed on 2D cultures and 3D cultured cell have been shown to be more persistent against cytotoxic compounds (3), low ethanol concentrations in 2D cultures with physiologically relevant cell types feature negative effects considering susceptibility to viral infections (46).

The evaporation methods utilized in previously mentioned studies feature rotavapor technique (10) and boiling the ethanol away (12). While both methods reportedly achieve low ethanol concentration in the final product, there are problems associated with these approaches.

Rotavapor equipment is a closed system where substitution of evaporated water and ethanol is technically challenging. If the vessel is rotated during processing, film coating may form on the vessel walls.

Increase in the temperature of the mixture to 80°C or higher may occur by intentional heating or by rapid accumulation of heat released in a low water:TEOS reaction. Both cases present a possibility of unwanted interactions that may result in an off-yellow color of the sol and possibly altered structure of the particle aggregates. While the origin of this effect is not known, interactions between silicic acid species and ions originating from mineral acids used to adjust pH are one possibility. (15)

Polyglyceryl silicates (PGS) could be used as alternative precursors due to their favorable properties in terms of reaction products (47). However, they are not commercially available and need to be synthesized separately.

If the gel would be used for testing cytotoxicity of pharmaceuticals or generic chemicals any effect caused by encapsulation material should be identifiable, controllable and even better, removable. With these considerations it is rational to remove the alcohol from the sol prior to use.

4.6.2 Nanoparticle toxicity

While silica has been approved for use in food and animal feed, questions about potential toxicity of silicate species has remained a matter of research and discussion. Some examples of potential toxic effects and a current view on toxicity of nanostructured silica is presented in this chapter.

Silica nanoparticles can be more harmful to cells that undergo slower division: analyzing cell membrane damage with lactate dehydrogenase assay indicates that rapidly dividing tumor cells are less affected than slowly dividing fibroblasts. (48) The effect may be caused by more extensive interaction of silanol groups present on silica particle surface with cell membranes over the course of time.

Amorphous silica particles of >100 nm diameter have been shown to induce hemolysis in blood cells (49). Further studies indicate that changes in the pore structure during aging, *i.e.* dissolution of surface molecules without re-condensation, induces higher quantity of hemolysis. This effect can be reduced by modifying silica particles with PEG coating. (50) The effect of modification by

addition of PEG may be explained by results discussed in (51) where encapsulation of silica particles inside PEG-covered “capsule particles” is deduced from rheological and AFM observations. While aggregate particle surfaces are considered to contain exposed silanol groups (8), it could be claimed that preventing direct contact of these chemical species with cellular membranes is beneficial for maintaining cellular integrity.

Monodisperse and stable silica nanoparticles have been studied for potential applications of gene delivery. They have been found to be able to induce specific protein silencing without significant cytotoxic effects. (52) A recent review by Fruijtier-Pölloth (2012) concludes that although *in vitro* models indicate some toxic properties for synthetic amorphous silica particles, only reported *in vivo* results show either inflammatory response following inhalation or lung embolisms following intravenous injection of high doses. (53)

The challenge in examining toxicity of any chemical species with *in vitro* models and extrapolating the results to *in vivo* is even more eminent with scarcely soluble silica. Supersaturated conditions may exist in *in vitro* conditions and silica concentration in cellular microenvironment may remain constant over a period of time. By contrast, *in vivo* systems exhibit constant exchange of fluids by means of blood flow. This results in a situation where localized silica aggregates experience dissolution and removal of dissolved products without accumulation in kidneys or other tissues. (53)

4.6.3 Sol stability

Metastability of acidic sols reduces the shelf-life of produced material. Base stabilization is an established technique for stabilizing colloidal silica sols and such products (*e.g.* Ludox) are available in a variety of particle sizes and concentrations (8) (54). Base stabilization is based on mutual electrochemical repulsion of condensed silica particles in absence of dissolved salts. Particle growth occurs by means of monomer addition to condensed clusters rather than fusion of clusters. The end result is a colloidal sol containing relatively large

(>100 nm) particles with a narrow size distribution. Gelation can be induced by salt-ion driven reduction of the water double layer surrounding particles.

While sols produced via base catalyzed hydrolysis are an attractive alternative because of their stability, the potentially large size of particles and the resulting structure of the gel may not be suitable from cell encapsulation perspective. Viscoelastic characterization of base-catalyzed silica gels suggests that they do not feature a spanning cluster formation as acid-catalyzed gels but rather structures that are better described as coagulated and loose (51).

While condensation and aggregation are temperature dependent reactions, it is not viable to freeze the sol in order to suspend these processes. Primary solvent in the sol at hand is water. Crystallization of water molecules upon freezing forces condensed particles together, whereupon they flocculate (54). Instead of forming a gel-like structure the result is a suspension of coagulated flake-like particles that are so large (1 mm) that upon thawing of the solvent phase they sediment. Although acidic sols at pH of 2.5-3.5 have been found to resist coagulation through freeze-thaw cycles, the method requires flash freezing to below -55°C and rapid thawing which both elude appeal from practical perspective. (54)

In a dilute sol with water content of 95-99 % condensed particles and particle aggregates are sparsely distributed. As object movement in the fluid is driven by Brownian motion, reducing the temperature of the sol also reduces the probability of particle or aggregate collision and condensation.

5 EVAPORATION PROCESS

Evaporation is the vaporization of a liquid that occurs only at the surface of the liquid. Physically vaporization occurs when molecules have enough kinetic energy or speed, *i.e.* the temperature is sufficiently high that the collision of one molecule to another at the liquid-gas phase boundary[5] results in shift of the receiving molecule from liquid to gas phase. Evaporation occurs almost in any temperature. Since temperature is only a statistical description of the average kinetic energy of particles in bulk material, some particles can have enough energy for evaporation even if the bulk temperature is relatively low.

In a closed system evaporated molecules accumulate in the gas phase and condensation of molecules back into the liquid phase occurs. In a state where the rate of evaporation and condensation are the same the gas phase is saturated. This is called equilibrium state. In binary systems the composition of equilibrium depends on the molar fraction of individual components.

In an open system where the headspace of liquid phase is freely exchanged the composition of equilibrium is not relevant. However, in a binary system at a constant temperature and total pressure the driving force for evaporation of a component from is the partial pressure of said component.

The driving force for evaporation is vapor pressure of a liquid substance. Consider the phase change of a liquid to gas as chemical reaction:

$$A(l) \leftrightharpoons A(g) \qquad \text{Eq. 5.1}$$

The equilibrium state is described by vapor-liquid distribution ratio *K*. The concentrations in liquid and gas phases can be denoted as *x* and *y*. *K* is then defined:

$$K = \frac{y}{x} \qquad \text{Eq. 5.2}$$

[5] Strictly speaking there is not exact boundary between the two phases. Instead there is a region where the transitional phase is not liquid or gas. This is called a Knudsen layer, and in normal conditions for a water-air boundary it is only a few molecules thick. This condition is not relevant for examining mass transfer phenomena in larger scales but the existence of such phenomena is necessary to recognize.

For binary systems a parameter called relative volatility α can be calculated. The parameter is defined as a ratio of vapor-liquid distribution ratios the two components in a binary system:

$$\alpha = \frac{K_i}{K_j} \quad \text{Eq. 5.3}$$

Raoult's law can be used to estimate the vapor pressure of solution when ideal behavior is presumed. The partial vapor pressure of a component is the product of the mole fraction x_n and vapor pressure of a pure substance p_n^*.

$$p \approx xp^* \quad \text{Eq. 5.4}$$

Vapor pressure of a pure substance, p^*, is determined by temperature. Equilibrium vapor pressure at a certain temperature can be estimated using an Antoine equation:

$$\log p^* = A - \frac{B}{T + C} \quad \text{Eq. 5.5}$$

Where A, B and C are experimentally derived constants. The values of the constants depend on the units that are used in the set of experimental data from which the parameters are derived. For water and ethanol the following constants can be used:

Table 5.1: Antoine equation constants for ethanol and water. P=bar, T=K

	A	B	C	T range	Source
EtOH	5.24677	1598.673	-45.424	292.77-366.63 K	(55)
H_2O	6.20963	2354.731	7.559	293-343 K	(56)

Changing the pressures in Eq. 5.4 with fugacities, f, f^* would take into account real behavior of substances. The relation of vapor pressure and fugacity is the dimensionless fugacity coefficient, $\phi = \frac{f}{p}$. For an ideal substance fugacity and vapor pressure are the same and the value of the coefficient is 1. For real substances in normal conditions fugacity coefficient is often other than 1. but approaches the value 1 as temperature or pressure is lowered.

Raoult's law states that the total vapor pressure p_T is the sum of partial vapor pressures of each component:

$$p_T = p_A + p_B \quad \text{Eq. 5.6}$$

The molar fraction of a component in the vapor is the product the ratio for pure vapor pressure to total pressure and molar fraction in liquid:

$$y = \frac{p^*}{p_T} x \quad \text{Eq. 5.7}$$

The rate of evaporation is dependent on temperature. Higher temperature translates to higher vapor pressure, which in turn is the driving force of evaporation.

As a surface phenomenon the rate of evaporation is also dependent on the area of the phase boundary surface. Whereas boiling occurs throughout the liquid volume, evaporation requires that liquid and gas phase are in contact.

At a constant temperature gas phase pressure also has an effect since high concentration of molecules above the liquid surface inhibits the escape of molecules from the liquid.

The concentration of evaporated molecules in the gas phase, *i.e.* the degree of saturation, has an effect on the rate of evaporation. If the gas phase is saturated, meaning two phases are at an equilibrium, there is no change in the bulk concentration of either phase. In terms of water it is possible to achieve equilibrium with ambient air.

The concentration of ethanol in the atmosphere has been estimated to be 71 pptv the 0-2 km layer above continents (57). In the process the liquid phase is exposed to ambient air, meaning that all evaporated ethanol is likely to become diluted very fast and that no condensation occurs in the reaction vessel. The driving force for ethanol evaporation is therefore the concentration of ethanol in the liquid phase.

6 ETHANOL QUANTIFICATION

Available methods for ethanol quantification consist of enzymatic and chromatographic methods. Additionally physical methods such as density or osmolality determinations are available. A headspace gas chromatography (HS-GC) method was adapted for the analysis in this thesis. The method was originally described for the analysis of ethanol from fermentation liquor (17).

While enzymatic methods are technically easier to conduct, several properties of the sample material advocate the use of a chromatographic method. The sample has a low pH and particles which could interfere with or inhibit proper functioning an enzymatic assay. While adjusting the pH is possible, it causes gelation which could, again, interfere with the assay. In addition to this some of the samples gel autonomously due to lag in sample processing. Enzymatic methods also have a relatively narrow linear range of operation. This necessitates preparation of dilutions when analyzing samples with a wide range of predicted concentrations. Even if the effect of particles in the sample could be normalized it would have to be done to all concentrations resulting from different dilutions.

Capillary gas chromatography is a chromatographic method that is based on different elution rates of gaseous analytes. The solid phase in gas chromatography can be a liquid or a solid material that is distributed inside a capillary structure. Typical method for introducing the sample to the capillary column is quickly evaporating a volume of solvent in which the analyte is dissolved in. However, if the sample liquid contains solid particles or compounds that do not evaporate, introducing these to the injection chamber or the column may result in damage or inaccurate results. To address this issue, *i.e.* analyzing evaporating compounds from samples that contain solids without additional processing, static headspace sampling can be applied. (58)

6.1 Static headspace sampling

Static headspace sampling is a sampling method where the sample is contained in a sealed vial that is subjected to temperatures that cause evaporation of analyte compounds. A sample of the gas phase is then extracted and injected to the column for analysis. (58)

Mass transfer of evaporating compounds in GC follows Henry's law (Eq. 6.1).

$$H = \frac{c_g}{c_l}, c_g = \frac{H}{1+H} c_0 \qquad \text{Eq. 6.1 (17)}$$

Where H is the Henry's constant, c_g and c_l are concentrations of the analyte in the gas and liquid phases and c_0 is the concentration of the analyte in the sample. Based on Eq. 6.1 the concentration of analyte could be determined by analyzing the headspace gas. However it is possible that the sample matrix leads to a difference in the value of *H* for each case. Internal standard calibration could be done by spiking samples with known quantities of analyte, but this approach is not efficient for repeated analysis or batch analysis. (17)

Full evaporation headspace sampling has been applied to overcome the challenge presented by matrix interference. The method utilizes complete evaporation of aqueous samples by equilibrating a small sample quantity in a headspace sampling vial at temperatures above normal boiling point of analyte and solvent. This results in practically full mass transfer of the analyte from sample matrix to gas phase. However, optimization of sample size, equilibration time and equilibration temperature is necessary to avoid saturation and incomplete mass transfer. (17)

6.2 Analyte detection

When quantifying ethanol, flame ionization detector (FID) can be applied for quantification. FID is based on increased convection of electrical current when ionized molecules are placed between two electrodes. FID requires that the sample contains combustible carbon compounds. The method is not able to distinguish isomers, *i.e.* compounds with the same formula but different

structure (*e.g.* dimethyl ether would not be distinguishable from ethanol). However the method is very sensitive and has a broad linear region of response. (58) This enables good usability in analysis of ethanol from aqueous silica sol as the only evaporating components are ethanol and water, of which the previous one is hardly detected. While silicic acid and silicates also evaporate, the temperatures that are required are considerably higher than for water or ethanol.

6.3 Signal analysis

The signal is obtained by automatic integration of the analyte signal peak, which has a value in pA proportional to the analyte concentration *c*. The peak is integrated over a time period *t* according to the parameters of the integrator. The resulting area of a peak *A* is expressed in pAs. When several samples with known mass *m*, weighed in milligrams, are subjected to analysis the variation between individual samples can be standardized by dividing the signal with the mass of specific samples. The resulting value is denoted relative signal *rs* (Eq. 6.2).

$$rs = \frac{s}{m} = \frac{[pA \cdot s]}{[mg]} \qquad \text{Eq. 6.2}$$

An external standard is used to calculate the analyte concentration in sample. Since FID response is linear to analyte concentration, linear regression is used to fit the standard points with a line. The equation of the line (Eq. 6.3) can then be solved for calculating analyte concentration (Eq. 6.4).

$$y = ax + b \qquad \text{Eq. 6.3}$$

$$x = \frac{y - b}{a} \qquad \text{Eq. 6.4}$$

When standard constituency is originally known in w-%, the result from solving Eq. 6.4 also results in a value with the unit w-%.

7 MATERIALS AND METHODS

7.1 Production of silica sol

Silica sols were produced by acid catalyzed hydrolysis of TEOS (98 %, Sigma Aldrich) with water that had resistance of 18.2 MΩ (MQ-water) (Millipore Milli-Q water purification system). Water:TEOS -ratio for hydrolysis mixture was 50. 1M hydrochloric acid (HCl) was added to achieve concentration of 0.01 M from total reaction volume. Batch size varied between 100 mL and 160 mL. All process phases were conducted in a ISO class 5 vertical laminar air flow cabin (Kojair) with HEPA filtered air flow of 0.45 m/s.

The reactor assembly consisted of one 600 mL decanter glass that was placed inside a plastic 1000 mL decanter. Two pieces of silicone tubing kept the glass decanter at a fixed height from the bottom while tape held the top lips of the vessels fixed. The top part of the glass decanter was wrapped with bubble plastic to act as a gasket. Two silicone tubes, supported by static supports, ran between the two decanters into the volume between them. The void was filled with approximately 200-250 mL of water that was circulated by a peristaltic pump (Watson Marlow, 505s) through an aluminum coil which was placed in a water bath (Braun Medical, Thermomix 1420). The decanter assembly sat on top of a magnetic stirrer and a scale (Mettler Toledo, BB2400). The magnetic bar had a length of approximately half of the inner diameter of the reaction vessel. Speed of the magnetic bar was adjusted so that it was high as possible without causing splashing of reaction mixture. The used equipment was sufficient to induce dispergation of TEOS and water.

During hydrolysis water was not circulated in the “jacket”. Temperature of the hydrolysis mixture was followed with a digital thermometer held in place by a static support. Heat generated in hydrolysis was detected as an increase in the temperature of the reaction mixture. Typical increase was in the range of 2 to 4°C, most commonly 3°C. Phase separation became undetectable typically after 20 to 30 minutes, most often at 25 minutes. Phase separation was

detected visually by assessing the clarity of the mixture. Hydrolysis was carried out for 40 to 50 minutes, most often 40 minutes. Hydrolysis was followed immediately by evaporation.

7.2 Evaporation process

Prior to evaporation the water bath was set to a temperature high enough, approximately 70 to 75°C, to heat the sol in approximately 10 minutes after turning on the circulation and maintaining a temperature of 60°C. The pump was operated at 140 rpm, which resulted in a volumetric flow of 455 mL/min with the used tubing. This corresponded to approximately a little more than two jacket volumes per minute.

Mass transfer was tracked gravimetrically. The scale was tared after sol had reached temperature of 50 to 55°C. Reason for this was heat expansion of silicone tubing that caused additional pressure on the scale.

Sampling was done by transferring 250 to 500 µL of sol into a 1.5 mL centrifuge tube which was immediately closed. Sampling interval varied between 10 and 60 minutes. Larger intervals were used to reduce analysis workload. Samples were stored in room temperature prior to analysis.

Evaporated water and ethanol were replaced with water at approximately 10 minute intervals. Replacement or compensation was done either by adjusting mass deviation to zero or higher.

Duration of evaporation varied from 90 to 180 minutes. The duration was counted from the moment the pump was turned on. Effective evaporation time was counted from the moment when sol temperature reached 50°C.

After evaporation the pump was stopped and the aluminum coil was transferred to ice. The pump was then turned on again and the ice was stirred to ensure continuous contact of coil and ice. After sol temperature had dropped to or below room temperature the sol was collected. For all but the first batch (see

section 7.6) the volume was adjusted to original batch volume to compensate any loss of volume during the evaporation.

Sols were filtered with a 0.22 µm filter (Millipore) prior to storing in a refrigerator held at +5-6°C. The purpose of this was to remove possible particle and microbial contaminants. Filtration did not affect dry matter concentration in a detectable way, as determined by parallel dry weight determinations from unfiltered and filtered sols.

7.3 Dry weight analysis

The dry matter content of the sols were analyzed by weighing two to four replicates of 1 mL on to a pre-weighed aluminum dish with an analytical scale (Sartorius A200S). The samples were dried in an oven at 105°C overnight (16-24 hours). The dried samples were quickly weighed. Weighing results were used to calculate dry weight percentage *dw%* according to Eq. 7.1.

$$dw\% = \frac{m_3 - m_1}{m_2 - m_1} * 100\ \% \qquad \text{Eq. 7.1}$$

Where m_1 is the weight of the dry vessel, m_2 is the weight of the vessel with the sample and m_3 is the weight of the dry matter and the vessel. Average, standard deviation and relative standard deviation were calculated for replicates.

7.4 Headspace gas chromatography

Standards were prepared by mixing absolute ethanol (Etax Aa, 99.5 w%, Altia Oyj) with MQ-water to achieve ethanol solutions with desired w%. Standard volumes were initially 10 mL but later volumes of 100-1000 mL were used.

Samples were transferred with a pipette (liquid samples) or a spatula (gelled samples) to a 20 mL headspace vial and weighed with an analytical scale (Mettler Toledo AX205). The approximate sample size was 40 mg, the mass of each sample being recorded separately. The vials were sealed with a manual crimper immediately after weighing.

Analysis was conducted with gas chromatography (Agilent 6890 N) equipped with headspace sampler (Agilent 7694) and operated with GC Chemstation software. GC was equipped with a capillary column (Agilent HP5) and a flame-ionization detector. The column was roasted at 240°C for 5 minutes prior to equilibration at 30°C. Equilibration was continued until a consistent background level of approximately 2 pA was achieved. Parameters of gas chromatography runs are presented in Appendix 0.

A system test was conducted by serially analyzing six replicates of a standard sample. Average, standard deviation and relative standard deviation of replicates were calculated to estimate reproducibility of the analysis. Linear standard curve was fitted to analysis results with MS Excel. Curve parameters were used to calculate the concentration of ethanol in samples according to Eq. 6.4. Samples were analyzed batch-wise in chronological order. The area was recorded and normalized according to Eq. 6.2.

7.5 Data processing

For each batch the results of ethanol analysis were arranged to match their respective samples. Duration of evaporation was adjusted to match processing time at or above 50°C. Regression analysis was conducted with MS Excel.

7.6 Batches

Seven R50-batches out of a total 14 batches (R20-76) were subjected to sampling and analysis.

Table 7.1: Batches produced

	Volumes (mL)		Evaporation time (min)	
Batch id.	Batch	Final	Nominal	Actual
131011 R50	100	91	90	86
191011 R50	150	150	120	115
181111 R50	150	150	180	170
231111 R50	150	150	120	110
081211 R50	150	150	180	168
090112 R50	160	160	120	113.5
110112 R50	150	150	120	116.5

7.7 Improvised observation of maturation

Maturation of the sol was examined qualitatively by repeating an improvised procedure for one batch over the course of four weeks. Samples from batch 081211 R50. stored in 5°C, were mixed in a 1:1 ratio with 5°C RPMI 1640 25 mM HEPES (Gibco) medium supplemented with 10 % FCS (Gibco) and 1 % PenStrep (Gibco) in a transparent plastic cuvette. Absorbance of the mixture was measured every 10 seconds for 30 minutes with a spectrophotometer (Shimadzu). Absorption was measured at a wavelength of 980 nm as the sol was found to have a maximum absorbance peak in this region.

8 RESULTS

8.1 Hydrolysis and evaporation

8.1.1 Temperature control

Temperature was monitored during hydrolysis and evaporation phases. Temperature control with improvised water jacket was fast and stable. Temperature profile for a typical batch from the beginning of hydrolysis to the end of evaporation is presented in Chart 8.1. While quality of data does not allow quantifiable analysis, slight increase in temperatures towards the end of the phase was observed. This occurred even though temperature of the circulating water bath was kept constant and water at room temperature was added during the process. This can be attributed to the reduction in energy consumption from reduced evaporation of ethanol towards the end of the phase.

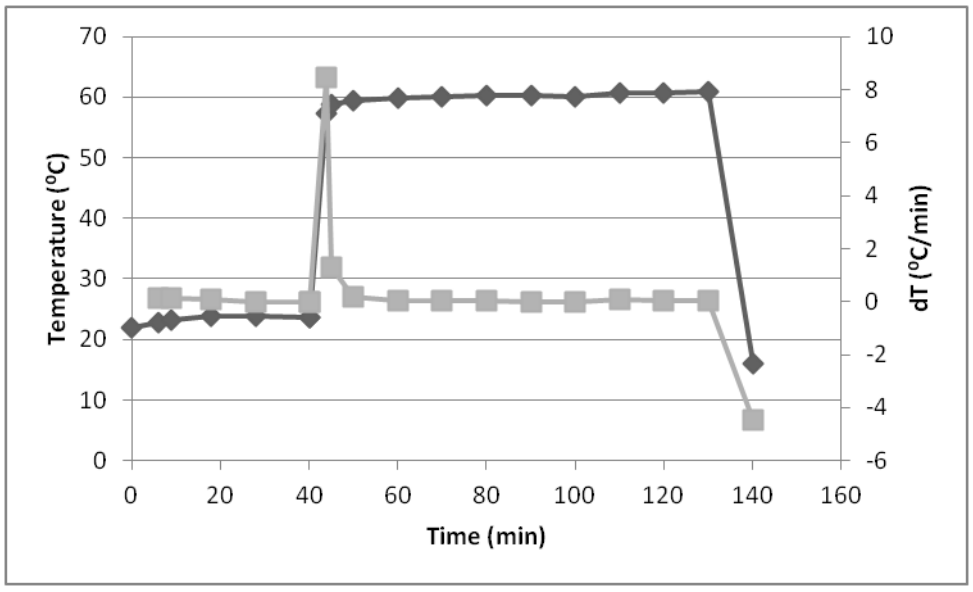

Chart 8.1: Example for batch temperature profile (black diamonds, left axis) and rate of temperature change (gray squares, right axis). Data from batch 131011 R50.

Average maximum rate of temperature increase (dT/dt) after the circulation pump was switched on was 5.22°C/min, with highest values approximately 8.5°C/min. Large standard deviation of 2.5°C/min in this data is attributed to

different observation time points for different batches - while processing temperature may have been reached it was not recorder until later. Altogether the water jacket provides a rapid and stable method for temperature control. A compilation of batch temperature profiles is presented in Chart 8.2. While batch-to-batch reproducibility is only at moderate level in the presented data, in principle the process could be considered reproducible.

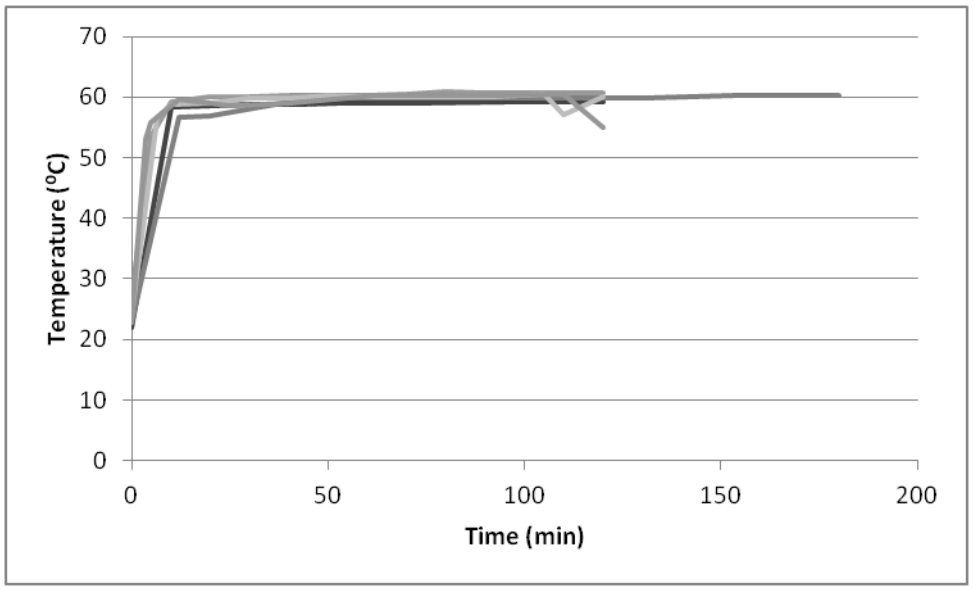

Chart 8.2: Stability of temperature during evaporation. Data from all batches, 131011 R50 excluded.

8.1.2 Water addition

The number of samples, scale readout and quantity of added water was recorded for calculating bulk mass transfer. Mass of sol at time *t,* m_t, after sampling and water addition was calculated according to Eq. 8.1.

$$m_t = m_r - m_s + m_{H_2O} \quad \text{Eq. 8.1}$$

Where m_r is the readout from the scale, m_s is the approximation for sample mass and m_{H_2O} is the mass of the added water.

Change in mass between two measurement points, dm, was calculated according to Eq. 8.2.

$$dm = m_{r,t_2} - \left|m_{t,t_1}\right| \quad \text{Eq. 8.2}$$

However, this parameter does not describe mass transfer caused by evaporation alone as also loss of mass from sampling is included. Adding the approximated mass of the sample to the equation gives dm_e that describes the mass transfer caused by evaporation alone (Eq. 8.3).

$$dm_e = m_{r,t_2} - \left|m_{t,t_1}\right| + m_{s,t_2} \quad \text{Eq. 8.3}$$

Plotting cumulative sum of absolute values of dm_e (Eq. 8.4), $\sum dm_{e,t}$ against evaporation time reveals a trend that can be described by a linear model. Example of this model is presented in Chart 8.3.

$$\sum_{t=0}^{n} dm_{e,t} = dm_{e,0} + dm_{e,1} + \cdots + dm_{e,n} \quad \text{Eq. 8.4}$$

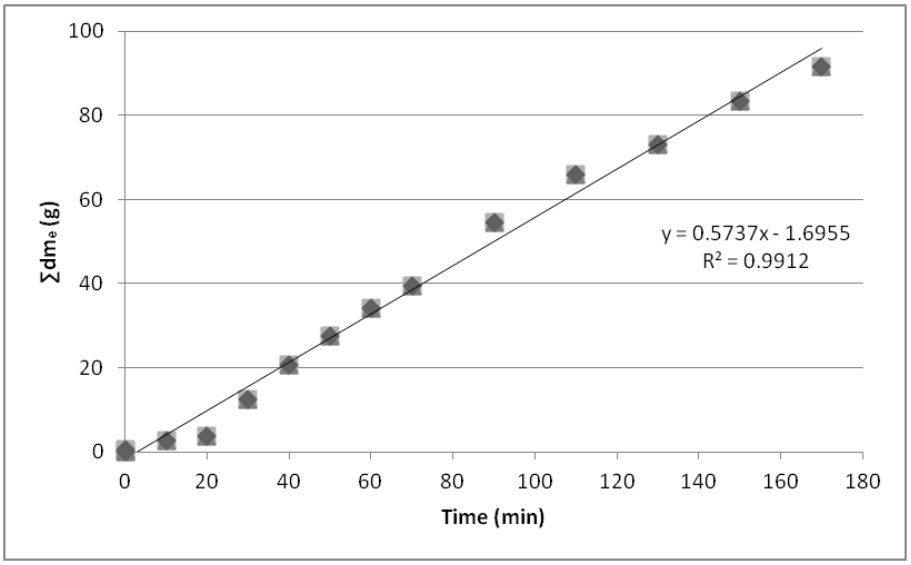

Chart 8.3: $\sum dm_e$ as a function of evaporation time. Data from batch 181111 R50.

Total mass of added water was normalized to batch size by dividing the total mass by approximation of batch mass (Eq. 8.5). The data is presented in Chart 8.4.

$$m_{w,n} = \frac{m_w}{m_b} \quad \text{Eq. 8.5}$$

Cumulative proportional mass of added water was calculated by dividing the cumulative amount of added water at a certain time point by the total mass of added water (Eq. 8.6).

$$m_{w,n,t} = \frac{m_{w,t}}{m_{w,tot}} \qquad \text{Eq. 8.6}$$

Where,

$$m_{w,tot} = \sum_{t=0}^{n} m_{w,t} \qquad \text{Eq. 8.7}$$

and

$$m_{w,t} = \sum_{t=0}^{t} m_{w,t} \qquad \text{Eq. 8.8}$$

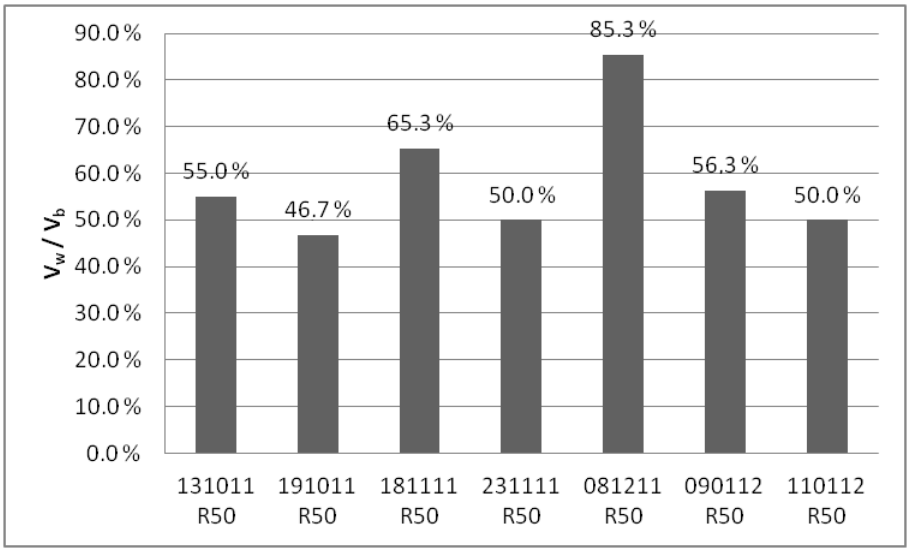

Chart 8.4: Water addition normalized to batch volume.

Batch size normalized rate of water addition was estimated by plotting cumulative proportional mass of added water against $m_{w,n,t}$ time (Chart 8.5).

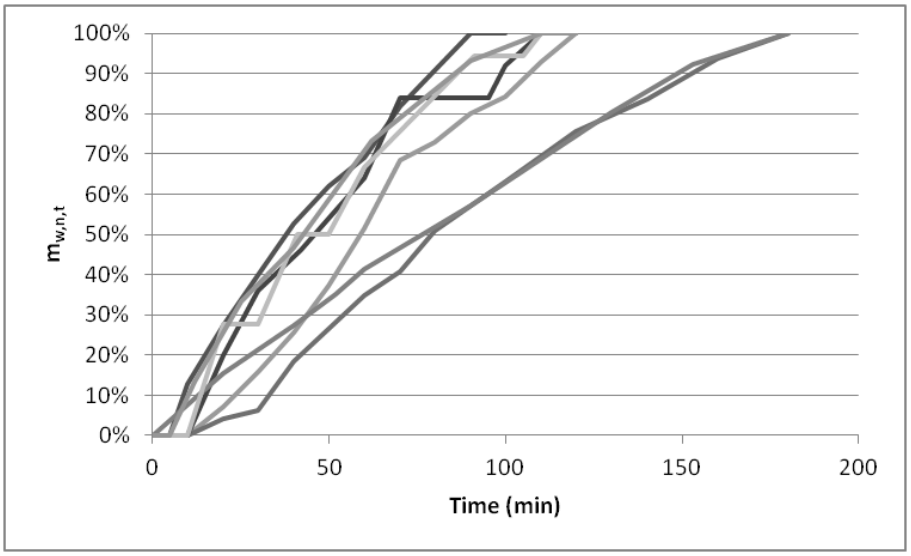

Chart 8.5: Batch size normalized data for addition of water during evaporation.

Regression analysis of entire data set presented in Chart 8.5 indicates that the average rate of water addition, $\frac{dm_{w,n,t}}{dt}$ is 0.884±0.186 %/min with average 0.973±0.016 for square of correlation coefficient R^2 (n=7). Splitting the data set according to evaporation time ($120 \leq t_e > 120$) gives more accurate description for the two batches with longer evaporation times. For $t_e > 120$ minutes, $\frac{dm_{w,n,t}}{dt}$ =0.592±0.038 %/min and R^2=0.989±0.005 (n=2) while for $t_e \leq 120$ minutes $\frac{dm_{w,n,t}}{dt}$ =0.945±0.084 %/min and R^2=0.967±0.014 (n=5). While this approach enables inter-batch comparison in terms of water addition when batch size varies, the difference in relative water addition rate caused by extended processing time is an indication of the downside of normalizing data. In other words, the lower rate for extended batches is because the normalized value $dm_{w,n}$, which has a maximum of 1. is distributed over a longer period of time.

8.2 Ethanol quantification

Reproducibility and linearity of HS-GC -method were good. Reproducibility was estimated by calculating the relative standard deviation (CV%) for the six replicates of a system test. Fit of standard curve to analysis of standard samples was evaluated with the square of correlation factor r, R^2. These indicators are presented in Table 8.1. Low CV% and high R^2 are characteristic

for reliable results. Linearity was established for maximum standard concentrations of at least 17 w-% when analyzing R50 sols.

Table 8.1: Relative standard deviations and squared correlation coefficients of standard curves for R50 batches.

Batches	CV%	R^2
131011 R50	3.30 %	0.9994
191011 R50	2.53 %	0.9895
181111 R50. 231111 R50	2.89 %	0.9972
081211 R50	0.49 %	0.9995
090112 R50. 110112R50	2.70 %	0.9996

8.2.1 Start- and endpoint analysis

Ethanol concentrations in the sols before evaporation, presented in Chart 8.6, indicate that theoretical maximum of 16.61 w-% is not present after hydrolysis. While a very interesting observation, the discussion of this matter takes place in section 0 and this section deals with analysis of evaporation rate.

Low concentration for batch 191011 R50 (Chart 8.6) may be the result of inefficient sealing of the HS-vial or a defect in the vial. It was noticed that some vials were not able to contain pressure during headspace equilibration because of damage to the lip of the vial. However, whether these specific vials were involved in that analysis is, even though a likely occurrence, not confirmed. In any case the reliability of results for batch 191011 R50 is questionable. For this reason those results are not evaluated for ethanol removal during processing.

The most diluted standard had concentration of 0.1 w-%. For batches 181111 R50 and 081211 R50 the final samples yielded signals lower than that of the smallest standard, *e.g.* $rs_{sample} < rs_{standard}$ for last samples in 081211 R50. Because of this, the end concentration for these batches is noted as 0.1 w-%.

While good linearity for standard determinations and curve was established, the detection limit of the method was not established separately. The background noise at the level of approximately 2 pAs was exceeded by the 4 pAs signal from the last sample of batch 081211 R50. While this low signal:noise-ratio

prevents its use in quantitative analysis, it is an interesting example of how sensitive the method could be.

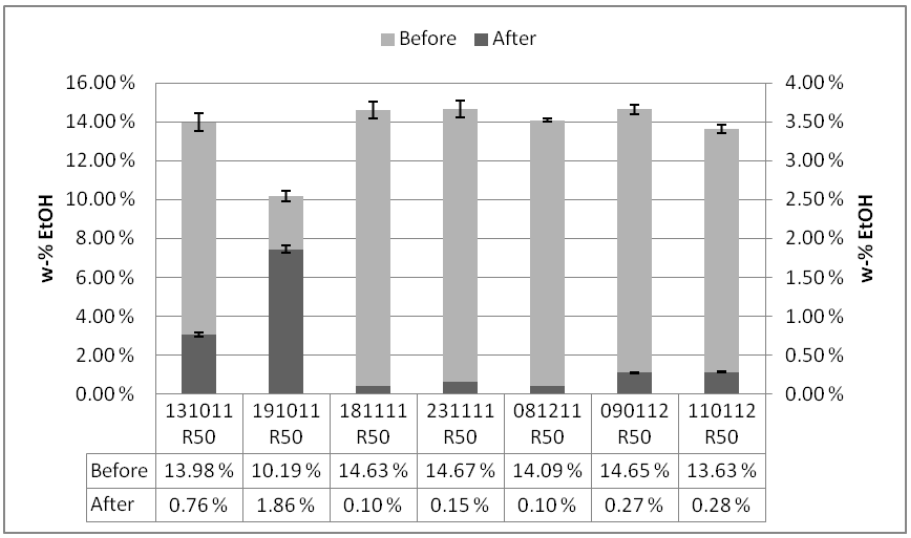

Chart 8.6: Ethanol concentrations for batches before (gray bars, left side) and after (black bars, right side) evaporation. Error bars represent ±1 product of relative standard deviation of the system test and calculated ethanol concentration.

Relative reduction in ethanol concentration and rate of reduction were calculated on the basis of determination results. As with water addition, normalization reduces amount of batch-specific detail available but serves as a way of comparing batches with different properties. Total relative reduction dE and rate of reduction as relative reduction per minute $\frac{dE}{dt}$ are presented in Chart 8.7.

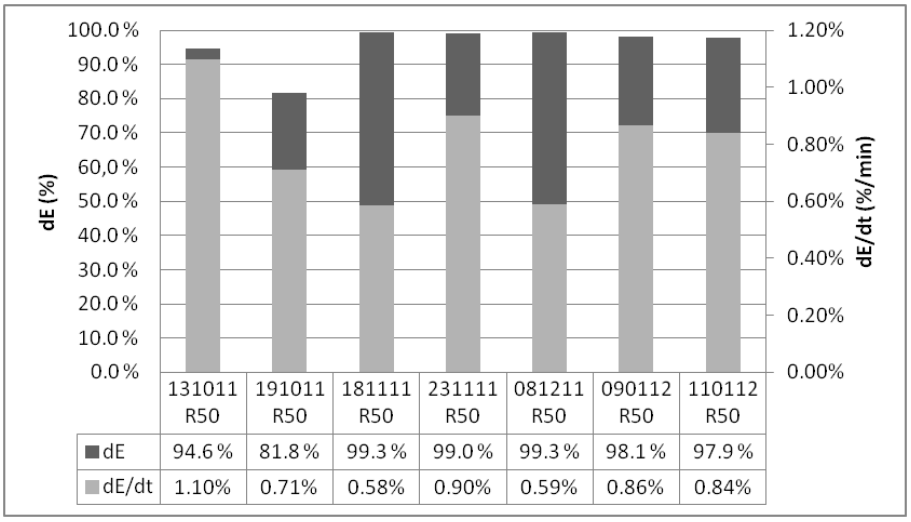

Chart 8.7: Total reduction and relative rate of reduction in ethanol concentration. All batches included.

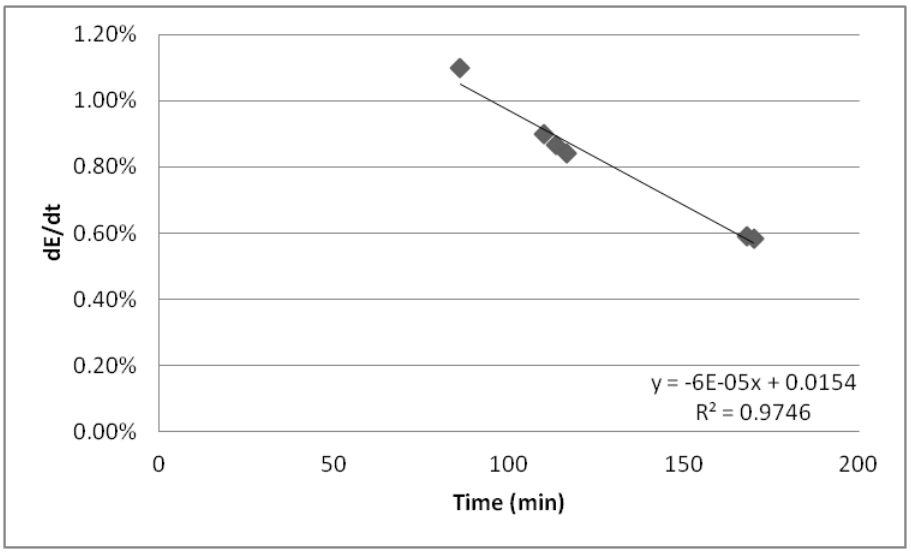

Chart 8.8: Rate of reduction in ethanol concentration as function of evaporation time. Batch 191011 R50 excluded.

Analyzing the relationship between rate of reduction $\frac{dE}{dt}$ and evaporation time t_e (Chart 8.8) shows a similar feature with rate of water addition. However, this is not only a feature induced by data analysis: overall rate represents an average rate, which does not reflect the actual dynamic nature of evaporation processes.

8.2.2 Evaporation curves

Ethanol quantification from different time points during evaporation phase shows an exponential reduction in ethanol concentration when processed at constant temperature. Example from one batch is presented in Chart 8.9.

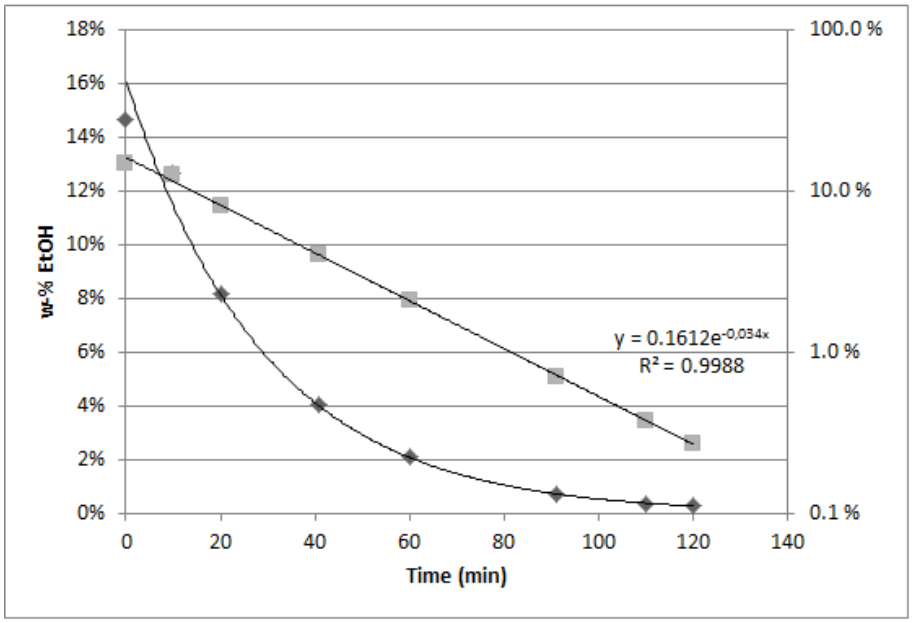

Chart 8.9: Evaporation curve for batch 090112 R50. Single data set represented on linear (black diamonds, left) and logarithmic (gray squares, right) y-scales. Exponential standard curve fitted in MS Excel, same curve for both scales.

To compare evaporation rates in different batches and to draw generalizations for optimizing duration of the evaporation phase, the data from different batches can be transformed into equations describing the development of ethanol concentration as a function of time.

Concentration data is linearized by calculating the logarithm of the w-% value. Parameters for the newly formed linearly correlated data are obtained using the SLOPE() and INTERCEPT() functions in MS Excel. RSQ() is used to evaluate the fit of the linear function to the data. The parameters correspond to constants *a* and *b* in Eq. 6.3, while $x = t_e$ and $y = \log[EtOH]$. Solving the equation for any $t_e \geq 0$ returns $\log[EtOH]$. Calculating the w-% can be done according to Eq. 8.9. The parameters for all batches, excluding 191011 R50. is presented in Table 8.2.

$$[EtOH] = 10^{\log[EtOH]} \qquad \text{Eq. 8.9}$$

Table 8.2: Linear equation parameters and squared correlation factors for logarithmic evaporation curve models.

Batch	131011 R50	181111 R50	231111 R50	081211 R50	090112 R50	110112 R50
a	-0.0147	-0.0175	-0.0174	-0.0195	-0.0151	-0.0149
b	-0.8655	-0.7430	-0.8640	-0.9421	-0.8693	-0.8277
R^2	0.9941	0.9973	0.9920	0.9935	0.9995	0.9984

A plot of the curves that are calculated from the models is shown in Chart 8.10.

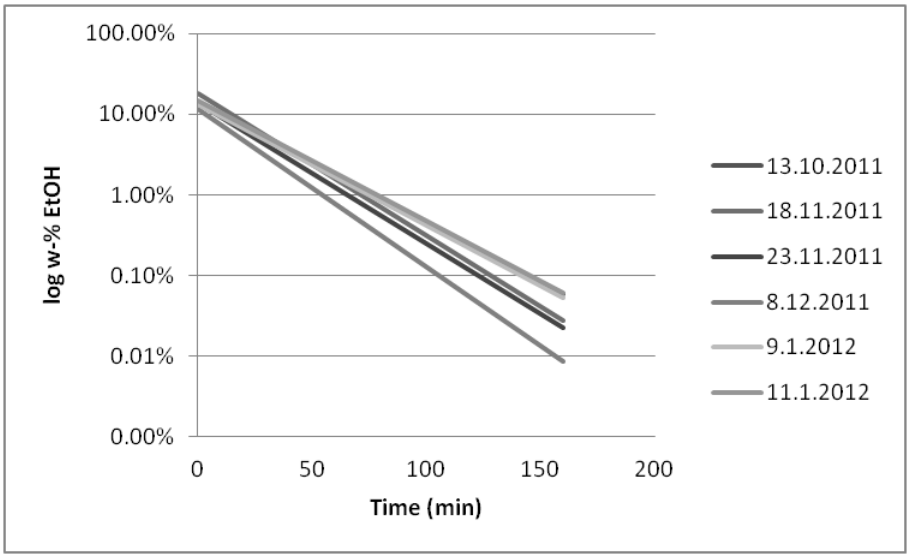

Chart 8.10: Lin-log plot of model-based evaporation curves.

The averages of model evaporation curve parameters are calculated to form a summary model. Model parameters are presented in Table 8.3 and the curve in Chart 8.11.

Table 8.3: Average model parameters

a	-0.0165
b	-0.8520
R^2	0.9958

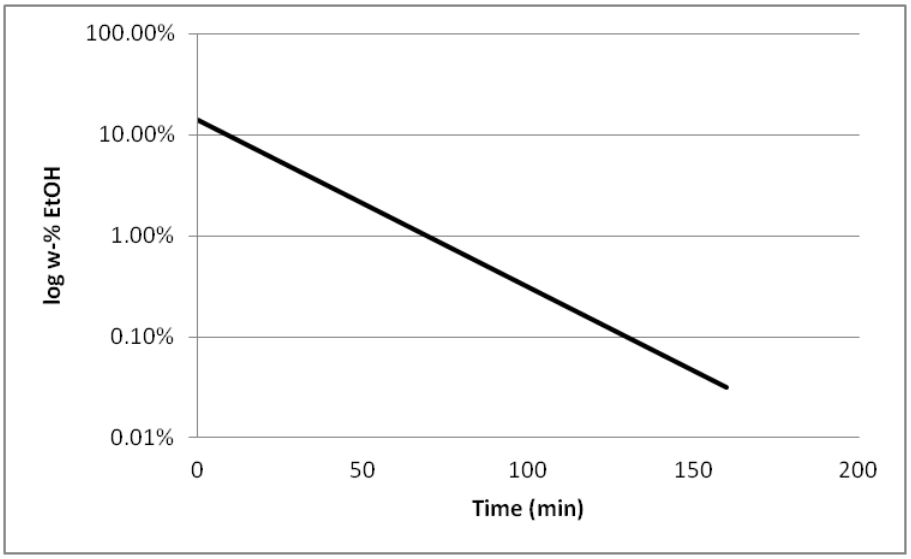

Chart 8.11: Average model for evaporation curve.

The average evaporation time to reach 0.1 w-% concentration can be calculated according to Eq. 8.10.

$$t_e = \frac{\log 0.001 - b}{a} \qquad \text{Eq. 8.10}$$

Average time based on parameters in Table 8.2 is 131.5 minutes. The time calculated from the average model parameters in Table 8.3 is 130 minutes. It should be noted that this time refers to processing at over 50°C.

8.3 Dry weight analysis

Sample volume was changed from 500 µL to 250 µL between batches 231111 R50 and 081211 R50. Lower results correlate with total volume of collected samples (linear regression, R^2=0.9436). In addition to different sample volumes, unintentional and undesirable thin film formation occurred during evaporation. Small rapid variations with air-liquid-glass interface level caused by mixing led to formation of a thin layer of condensed silica at the interface. This deposition may account for some of the variation in dry matter levels between batches. However, the extent of film formation was not measured and therefore it is not possible to state whether there is further correlation with the results of dry weight determinations.

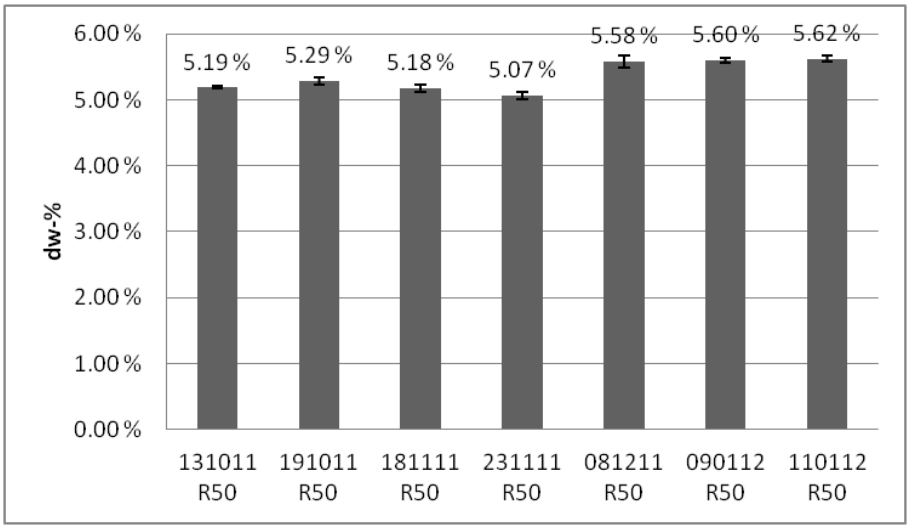

Chart 8.12: Dry weight content of produced sols. Error bars represent ±1 standard deviation of replicate analysis.

Average relative standard deviation (CV%) for replicate determinations (n≥3) was 0.95 % (n=6; min 0.35 %; max 1.63%). Results for determinations are presented in Chart 8.12.

Halving the sample volume for the three last batches resulted in higher dry matter concentrations as calculated SiO_2-concentration would suggest. The theoretical $Si(OH)_4$ and SiO_2 weight proportions in fully hydrolyzed and fully condensed sols are 8.66 % and 5.42 %, respectively. Lower and higher yields can be partially explained in terms of processing issues and a hypothetical feature of the dry weight analysis which is discussed further in section 9.

8.4 Maturation testing

Background absorbance caused by plasticware was taken into account by zeroing the spectrophotometer prior to measurements. Cell culture media was found to have no overlapping absorbance peaks.

The measurements suggest that although gel point is reached fairly quickly as indicated by tipping experiments, the structure changes at least for another 30 minutes. Absorbance measurements after neutralization and after 30 minutes waiting period are presented in Chart 8.13.

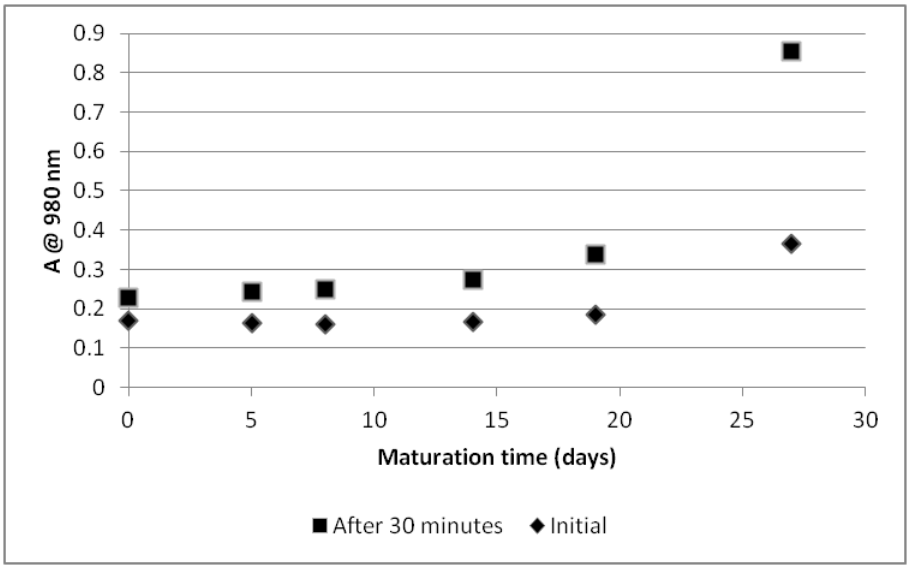

Chart 8.13: Absorbance measurements of silica sol mixed with buffered cell culture media. Absorbance was measured every 10 seconds for 30 minutes. Presented here are initial and last values as a function of maturation time in days. Absorbance was measured at wavelength of 980 nm.

While an increase in change of absorbance over a 30 minute period of gelation is observed for the first 19 days, the relative change is 3-fold at 27 days when compared to the change after 19 days. This suggests that t_{gel} decreases slowly at first, but towards the end of the shelf-life in shortens significantly. It should be noted that within the scope of this thesis there is not direct correlation to be presented between measurement data and actually measured t_{gel}-values. Additionally the method used to acquire the data presented here has not been tested before - the data is used to estimate degree of maturation qualitatively and is considered valid until other independent variable than maturation time can be accounted for the change in observations.

9 DISCUSSION

9.1 Material processing and properties

High temperature processing should be kept as short as possible to extend the shelf-life of the product. However, the processing time should always be the same as it affects the degree of condensation and aggregation in the product. Similarly the processing temperature and temperature profile should remain unchanged. These considerations coupled with data obtained from the batches produced for this thesis would suggest that to produce highly similar products from the same recipe, extending the evaporation time beyond that suggested by the experimental model would be necessary. This would ensure that the ethanol concentration at the end of processing would exhibit only very little variation.

Water addition is a matter that should be considered for further development in the current process. The optimum case would be that replacement water was added continuously to replace any evaporated solvents. However, while the process is conducted as manual labor this remains a labor-intensive approach that also suffers from the risk of operator error. This aspect should be kept in mind when examining the results presented in this thesis. Even if care is taken in recording measurements as accurately as possible there can hardly be the same level of accuracy or reliability as there would be with an automated logging system. Even though the results obtained by analyzing measurements conducted during the process have been presented as if there was a natural correspondence with a linear model, the complexity of mass transfer in a dynamic open system should be acknowledged. Some parameters, such as ambient pressure and humidity, that affect evaporation have not been included in the analysis of results.

The effect of silica in water-ethanol evaporation has not been addressed in the context of this thesis. The interaction between solvent molecules and dissolved or dispersed particles occurs partially through low-range attractive molecular forces. This means that some liquid molecules are less prone to escape from

liquid phase in spite of coming to the surface layer. In addition, when homogenous distribution of all molecules and particles in a dispersion is presumed, the extent to which solid particles occupy the liquid-gas interphase layer affects the total available surface area for liquid molecules to occupy. The fact is that the sol is a highly dynamic system with simultaneous condensation, aggregation and hydrolysis of colloidal species occurring at the molecular and particle level, *i.e.* simultaneous multi-level polymerization and Ostwald ripening. Due to this it is challenging to extend the hypothetical evaluation of solvent-particle interaction to more than a qualitative estimation of the degree to which evaporation is reduced by solids in the process.

While reliably achieving low ethanol concentrations is desirable, consideration should be given to achieving predictable and suitable gelling behavior in order to comply with the needs of cell encapsulation. For this purpose it is necessary to evaluate the effect of processing on the sol/gel properties. Acid catalyzed hydrolysis was the chosen method for producing a silica sol from an alkoxide precursor. While base catalyzed hydrolysis would yield a stable sol, large particle/aggregate size and the resulting different properties of the gel may be less suitable for cell encapsulation. Base catalyzed sols and gels have been reported to have a loose structure (51), which would presumably lead to different physical properties of the gel matrix. In some applications cell migration or proliferation could be guided via density gradients and thus heterogeneous structure might be purposeful. However, the benefit of potential reproducibility provided by the acid-catalyzed sol/gel pathway has been more significant within the scope of this thesis.

Maturation of the sol has been observed superficially and via an improvised method within this work. While lack of detail and proper analysis methods sets limitations on how much can be said about the effects of maturation on a quantitative level, it can be stated that there is a detectable change in the gelation time over a 29-day maturation period.

9.2 Processing equipment

The effect of ambient pressure variations within the 980-1030 hPa range also have an effect on evaporation in an open system. While temperature and relative ambient moisture have a more significant effect on the rate of water evaporation and thus the way in which the process is monitored, ambient pressure variations of 50 kPa may occur especially between the summer and winter seasons and the effect should be taken in to account.

Better equipment is a necessity when considering the possibility of validation. While the current study was only moderately affected by lack of automated data recording, the reproducibility of the process requires that the human link between signal detection and recording could and should be removed. In spite of applying highly rigorous discipline to measurement reading and recording to alleviate observer bias, the degree of accuracy and reliability that would be achievable with automated process measurements would outperform human operators considerably.

Pump control according to scale output would minimize vessel-phase interface level variation and generally support more repeatable processing. It would be possible to implement this in a sophisticated manner by adding a PI-controller or a signal filter between the scale output and pump input. A simple, even if less reliable, method would be to directly link scale output voltage to pump input to create a binary control of pump motor.

9.3 Analytical methods

The results of the dry weight analysis raise more issues than they provide answers. For example, previously presented observation suggested that the dried material does not consist only of SiO_2. This suggests that complete condensation into SiO_2 does not occur but that there remains -OH groups that contribute to increased mass of silica. Tetrahedral configuration of the central silicon atom could be considered to lead to a maximum of three Si-O-Si bonds for surface molecules on a particle. From this it could be hypothesized that the

distribution of silica species in dried samples is somewhere between 1:0 and 0.85:0.15 for SiO_2 and $Si(OH)_4$. *i.e.* fully condensed and not condensed at all. While it is unlikely that uncondensed particles remain in the dried sample this estimate could be stated more accurately in terms of $SiO_{2-x}(OH)_x$, which takes into account an assumed average of two bonds for every silicon atom. Additionally, it is possible that water and/or organic impurities are captured inside the shrinking gel structure and thus contribute to the overall mass of the sample after drying.

In addition to uncertainty rising from material properties, dry weight analysis conducted in this thesis also suffers from variability in the protocol according to which the determinations were made. However, more crucial is the question whether the used temperature is sufficient to remove moisture from a shrinking gel structure.

Theoretical ethanol concentration in a fully hydrolyzed R50 sol is 16.61 w-%. While negative deviation from this figure could be considered as an indication of incomplete hydrolysis, high R-values have been suggested to lead to rapid completion of the reaction and reaction mixture indicates peak hydrolysis rate to occur before half of the hydrolysis period has passed. Also, given the conditions during hydrolysis it is not likely that $Q_0(3.1)$ functionalized species are present in the sol at the end of the phase. Additionally, it is likely that any residual functional groups would be hydrolyzed during evaporation because of high temperature and removal of ethanol which further changes the stoichiometric balance towards products (Eq. 4.2).

Choice of system test sample should be taken into account when considering the reliability of endpoint measurements. The system test sample could be chosen arbitrarily, but typically a criteria of sufficiently high signal or a middle position in the standard set is used as basis for choice.

Effect of equilibration during sample storage could be considered when evaluating the results from HS-GC-analysis. Samples were stored in room temperature for variable times between sampling and analysis. It is thus very

likely that equilibration occurred between the gas and liquid phase in the sample container. However, the total container volume was 1.7 mL, meaning that between 15 and 30 % of the total volume consisted of the sample liquid. The pure vapor pressure of ethanol at 21°C is approximately 6600 Pa and when presuming that prevailing pressure inside the sample container is normal ambient pressure, *i.e.* 101325 Pa, the partition factor K (Eq. 5.2) is 0.065. With for example 14 w-% sample concentration the equilibrium would be 0.91 w-%, which in normal pressure and temperature and 1.2 mL headspace volume means the equivalent of $1.3*10^{-5}$ grams of ethanol out of total 0.07 grams in a 0.5 mL sample. This translates to 0.018 % of the total ethanol found in the sample.

Material characterization possibilities include small angle x-ray scattering (SAXS), direct light scattering (DLS), atomic force microscopy (AFM) and oscillating rheometer. Additionally several material characteristics can be determined by physical measurements. Dry matter content used in this thesis has been demonstrated to be only an approximate in terms of sol properties. While it is possible to use it as preliminary parameter when screening for formulations with desired properties, characterization of the material should be conducted with appropriate equipment. SAXS and DLS could be used to follow the evolution of particle and aggregate sizes in the sol without interfering significantly with the sample properties. This determination will be necessary when characterizing the stability of sols or when confirming process product properties. AFM can be used to characterize the gel structure produced through different formulations. While sample preparation required by the method may affect the acquired results to the extent that measurements do not reflect actual consistency of the gel and that the method provides information about the surface layer of the sample, AFM would be useful to determining effect of sol maturation on gel properties. If the degree to which sample preparation affects the gel structure are determined, AFM could be used to great extent in analyzing structural variation in different formulations.

The dynamic nature of the sol/gel system over maturation time, as detected by absorbance measurements, has direct implications in terms of sol usability - as t_{gel} changes over the shelf-life of the product the user must take this change into account in order to gain repeatable results. Methods already applied for determining gel time are rheological measurements with an oscillating rheometer and a rotational viscometer. While a rotating viscometer could be used to detect gelation, it does not allow for examination of gel properties far beyond gel point. An oscillating rheometer would provide insight into gelation and the development of gel properties, but even with it any statements that refer to the environment presented to the encapsulated cell must be drawn from indirect measurements.

It should be noted that evaporation of ethanol occurs also at room temperature, *i.e.* during hydrolysis phase. As ethanol is generated in the reaction the concentration gradient between the liquid and gas phases increases and the rate of evaporation increases as well. However, most mass transfer occurs during processing at increased temperature.

With Eq. 5.5 it is possible to calculate approximate vapor pressure for ethanol during hydrolysis and evaporation. At 60°C and 20°C p^* for ethanol is 49 and 6.2 kPa and *K* is 0.48 and 0.06. respectively. At a temperature of 20°C the relative volatility α of ethanol-water system is 2.596 and at 60°C 2.467.

Ambient moisture affects the volatility of water. This presents a problem for process control in an open vessel. Unless the process is undertaken in a controlled environment where air moisture is not affected by ambient moisture, the rate of evaporation for water is different at different conditions. While it is possible to measure and take into account variation in ambient pressure, the variations it may cause in processing time are not acceptable as the extent to which the material is different may be too great.

Evaporation is a surface phenomenon. The rheological behavior of a colloidal silica sol usually is, and was in this work, Newtonian, which means that mixing can cause the formation of a vortex. In practice this means that a surface

geometry of a flat disc is replaced with a funnel-like shape. This shape has higher surface area than a flat disc. While evaporation rate is limited by the available surface area, the effect of vortex formation should be taken in account. Preliminary calculations with process data included a parameter that described available surface area per unit of fluid volume. Recognizing the dynamic nature of the surface area led to the exclusion of this parameter as measuring the degree to which the surface geometry is changed was not conducted.

In the current process model evaporated ethanol is released to the atmosphere. This presents work safety related risks such as accumulation of ethanol vapor in poorly ventilated spaces to the extent that a fire hazard exists. While the quantities released vary depending on batch size and formulation, the current formulation releases at most no more than 27 grams of ethanol over a period of two hours. From an environmental point of view releasing ethanol into the atmosphere is not advisable as this may result in increased generation of ozone.

The material has relatively short shelf-life and a research project might require a long time to conduct. In order to compare measurements done to materials produced at different times the reproducibility of the process should be high. The same applies to possible products that are commercialized. In addition to controlling critical process parameters, secondary parameters such as stirring speed and shear forces caused by impeller geometry should be identified.

10 CONCLUSIONS

An overview of previous work done within the scope of the Cell-In-Gel project in terms of process development and subsequent development of the low-ethanol production process for acid catalyzed silica sols has been provided in addition to a description of the materials and methods. The rationale for removing ethanol from silica sols intended for cell encapsulation is that cells are sensitive to small concentrations of ethanol.

The described process equipment can be used to produce low ethanol silica sols through a simple process. However, the equipment sets limitations to the extent to which the process is repeatable. By compromising between extended processing time and reliability it is possible to remove ethanol to a 0.1 w-% concentration with a processing time of 130 minutes at 60°C. However, to account for variability in ambient conditions, extending the phase duration would probably result in less variation in terms of end product concentration.

Additional potential development objectives include a simple and effective method for confirming process product properties. The dry weight determination method used in this thesis has been shown to be simple, but somewhat lacking in detail when it comes to sol/gel properties on a smaller scale. Should the method continue to be applied in future projects, attention should be paid to the extent to which drying gels are able to retain water and other compounds within the matrix structure. Should the dry weight determination continue to see use for any reason, suitable development goals could be to determine the extent to which the dried sample weight changes if the drying period is varied between 12 and 48 hours or if the drying temperature is changed from 105°C to up to 300°C or more.

An improvised spectrophotometric method was used in this thesis to estimate the effect of maturation time on gelation time. While maturation time is considered to be the only variable explaining the observed changes, the gathered data provides the possibility for only qualitative examination. When combined with the need for alternative methods for determining process product

sol properties, the need for quantitatively examining gelation time and the properties of a gelated sol/gel raises a request for suitable yet affordable methods.

While the presented process can be used to produce material for cell encapsulation research, the highly dynamic nature of the material presents challenges for reproducible production. In addition it was found that the maturation time has an effect on the gelation time, the effect becoming more apparent as the sol matures further. Further work should focus on developing a more controlled, *i.e.* automated, process which could then be used to reliably produce materials for characterization of different formulations.

REFERENCES

1. *Encapsulation of cells within silica matrixes: Towards a new advance in the conception of living hybrid materials.* **Meunier, Christophe F., Dandoy, Phillippe and Su, Bao-Lian.** 2010. Journal of Colloid And Interface Science, 342. 211-24.

2. *Synthetic 3D multicellular systems for drug development.* **Rimann, Markus and Graf-Hausner, Ursula.** [ed.] Hal Alper and Wilfried Weber. 2012. Current Opinion in Biotechnology, 1-7.

3. *Three-dimensional chitosan scaffold-based MCF-7 cell culture for the determination of the cytotoxicity of tamoxifen.* **Dhiman, Harpeet K., Ray, Alok R. and Panda, Amulya K.** 2005. Biomaterials, 26. 979-986.

4. *Pancreatic cancer organotypic cultures.* **Froeling, F.E.M., Marshall, J. F. and Kocher, H. M.** 2010. Journal of Biotechnology, 148. 16-23.

5. *COUNCIL REGULATION (EC) No 440/2008.* **THE COMMISSION OF THE EUROPEAN COMMUNITIES.** Brussels : s.n., 5 30. 2008. Official Journal of the European Union, L142/1-739.

6. *High-throughput 3D spheroid culture and drug testing using a 384 hanging drop array.* **Tung, Y C, et al.** 2011. The Analyst, 136. 473-478.

7. *The third dimension bridges the gap between cell culture and live tissue.* **Pampaloni, Francesco, Reynaud, Emmanuel G. and Stelzer, Ernst H. K.** 2007. Nature Reviews Molecular Cell Biology, 8. 839-845.

8. **Brinker, C. J. and Scherer, G. W.** *Sol-Gel Science: The Physics and Chemistry of Sol-Gel Processing.* San Diego : Academic Press, Inc., 1990. ISBN-13: 978-0-12-134970-7.

9. *Silica sol-gel encapsulation of pancreatic islets.* **Peterson, C M, Pope, E J and Peterson, K P.** 1998. Proceedings of the Society for Experimental Biology and Medicine, 218. 365-9.

10. *Biocompatible Sol−Gel Route for Encapsulation of Living Bacteria in Organically Modified Silica Matrixes.* **Monte, Francisco del, et al.** 2003. Chemistry of materials, 3614–3618.

11. **Dickson, David J.** Photobiological Hydrogen Production from the Cyanobacterium Synechocystis sp. PCC 6803 Encapsulated in Sol-gel Processed Silica. *Dissertation, Doctor of Philosophy.* [PDF]. Maryland Heights : Oregon State University, 2011.

12. *Cell viability in a wet silica gel.* **Vallet-Regi, Maria, et al.** 2009. Acta Biomaterialia, 5. 3478–3487.

13. *Basic fibroblast growth factor- and platelet-derived growth factor-mediated cell proliferation in B104 neuroblastoma cells: effect of ethanol on cell cycle kinetics.* **Luo, Jia and Miller, Michael W.** 1997. Brain Research, 770. 139-150.

14. *Hyaluronic acid signals for repair in ethanol-induced apoptosis in skin cells in vitro.* **Neuman, Manuela G., et al.** 2010. Clinical Biochemistry, 43. 822-826.

15. **Jokinen, Mika.** E-mail exchange. Unpublished empirical observations suggest that irreversible chemical reactions occur in silica sols when heated to temperatures above 80 °C.

16. *Towards self-steered studies by working in R&D projects.* **Jokinen, Mika, Tuovinen, Minna and Villa, Karlo.** Turku, 2012. International Conference on Engineering Education.

17. *Rapid determination of ethanol in fermentation liquor by full evaporation headspace gas chromatography.* **Li, Hailong, et al.** 2009. Journal of Chromatography A, 169-172.

18. *Cell-matrix adhesions in 3D.* **Yamada, Kenneth M. and Harunaga, Jill S.** 2011. Matrix Biology, 30. 363–368.

19. *Basement membrane proteins: structure, assembly, and cellular interactions.* **Paulsson, M.** 1992. Critical Reviews in Biochemistry and Molecular Biology, 27. 93-127.

20. *Cellular Microenvironment Influences the Ability of Mammary Epithelia to Undergo Cell Cycle.* **Streuli, Charles H., Jeanes, Alexa I. and Maya-Mendoza, Apolinar.** 2011. PLoS One, 6. e18144.

21. *Hydrogels and microtechnologies for engineering the cellular microenvironment.* **Gauvin, R., et al.** 2011. Wiley Interdisciplinary Reviews. Nanomedicine and Nanobiotechnology.

22. *Cellular Encapsulation in 3D Hydrogels for Tissue Engineering.* **Khetan, Sudhir and Burdick, Jason.** 2009. Journal of Visualized Experiments, 32.

23. *Biophysical regulation of tumor cell invasion: moving beyond matrix stiffness.* **Kumar, Sanjay and Pathak, Amit.** 2011. Integrative Biology, 3. 267-278.

24. *Rapid Generation of Single-Tumor Spheroids for High-Throughput Cell Function and Toxicity Analysis.* **Ivascu, Andrea and Kubbies, Manfred.** 2006. Journal of Biomolecular Screening, 11. 922-932.

25. *Hydrogels for tissue engineering: scaffold design variables and applications.* **Mooney, David J. and Drury, Jeanie L.** 2003. Biomaterials, 24. 4337–4351.

26. *On the Use of Hydrogels in Cell Encapsulation and Tissue Engineering Systems.* **Thanos, Christopher G. and Emerich, Dwaine E.** 2008. Recent Patents on Drug Delivery & Formulation, 2. 19-24.

27. *Rational design of hydrogels for tissue engineering: Impact of physical factors on cell behavior.* **Goepferich, Achim, Sommer, Florian and Brandl, Ferdinand.** 2007. Biomaterials, 134-146.

28. *Multi-hierarchical self-assembly of a collagen mimetic peptide from triple helix to nanofibre and hydrogel.* **O'Leary, Lesley E. R., et al.** 2011. Nature Chemistry, 821–828.

29. *Requirement of basement membrane for the suppression of programmed cell death in mammary epithelium.* **Pullan, Shirley, et al.** 1996. Journal of Cell Science, 109. 631-642.

30. **Kleinman, Hynda K.** Preparation of basement membrane components from EHS tumors. *Current Protocols in Cell Biology.* 2001. 10.2.1-10.2.10.

31. *Matrigel: Basement membrane matrix with biological activity.* **Kleinman, Hynda K. and Martin, George R.** 2005. Seminars in Cancer Biology, 15. 278-286.

32. *Hyaluronan hydrogel: An appropriate three-dimensional model for evaluation of anticancer drug sensitivity.* **David, Laurent, et al.** Acta Biomaterialia, 4. 256-263.

33. **Glycosan Biosystems, Inc.** Hystem Hydrogel for Stem Cell Culture. *Glycosan Biosystems webpage.* [Online] [Cited: March 11. 2012.] http://www.glycosan.com/ha_products/hystem_kit.html.

34. —. Hyaluronan, Gelatin and Heparin sourcing. *Glycosan Biosystems website.* [Online] [Cited: March 11. 2012.] http://www.glycosan.com/ha_technical/extracel_component_origin.html.

35. *The effect of matrix characteristics on fibroblast proliferation in 3D gels.* **Rizzi, Simone C., et al.** 2010. Biomaterials, 31. 8454–8464.

36. *Reversible hydrogels from self-assembling artificial proteins.* **Petka, W. A., et al.** 1998. Science, 281. 389.

37. *Design of nanostructured biological materials through self-assembly of peptides and proteins.* **Zhang, Shuguang, et al.** 2002. Current Opinion in Chemical Biology, 6. 865-871.

38. *Primary sequence of ionic self-assembling peptide gels affects endothelial cell adhesion and capillary morphogenesis.* **Sieminski, A. L., et al.** 2008. Journal of Biomedical Materials Research A, 87. 494-504.

39. *Temperature and pH effects on biophysical and morphological properties of self-assembling peptide RADA16-I.* **Ye, Zhaoyang, et al.** 2008. Journal of Peptide Science, 14. 152-62.

40. *Designer Self-Assembling Peptide Nanofiber Scaffolds for Adult Mouse Neural Stem Cell 3-Dimensional Cultures.* **Zhang, Shuguang, et al.** 1. Cambridge : s.n., 2006. 1. p. e119.

41. *Recent bio-applications of sol–gel materials.* **Coradin, Thibaud, et al.** 2006. Journal of Materials Chemistry, 16. 1013-1030.

42. *Entrapment of viable microorganisms by SiO2 sol-gel layers on glass surfaces: Trapping, catalytic performance and immobilization durability of Saccharomyces cerevisiae.* **Diré, S., et al.** 1993. Journal of Biotechnology, 30. 197-210.

43. *Encapsulation of Hepatocytes by SiO2.* **Muraca, M., et al.** 2000. Transplantation Proceedings, 32. 2713-2714.

44. *Thermophilic Mixed Culture of Bacteria Utilizing Methanol for Growth.* **Snedecor, Bradley and Cooney, Charles L.** 6. Cambridge : American Society for Microbiology, 1974. Applied Microbiology, 27. 1112-1117.

45. *Ethanol Enhances Susceptibility to Apoptotic Cell Death via Down-Regulation of Autophagy-Related Proteins.* **Haefen, Clarissa von, et al.** 2011. Alcoholism: Clinical and Experimental Research, 35. 1381-1391.

46. *Ethanol enhances hepatitis C virus replication through lipid metabolism and elevated NADH/NAD+.* **Seronello, Scott, et al.** 2010. Jouranl of Biological Chemistry, 285. 845-854.

47. *Encapsulation of Biologicals within Silicate, Siloxane, and Hybrid Sol−Gel Polymers: An Efficient and Generic Approach.* **Gill, Iqbad and Ballesteros, Antonio.** 1998. 120. 8587–8598.

48. *In vitro cytotoxicitiy of silica nanoparticles at high concentrations strongly depends on the metabolic activity type of the cell line.* **Kong, Zwe-Ling, et al.** 2007. Environmental Science & Technology, 41. 2064-2068.

49. *Mesoporous Silica Nanoparticles for Reducing Hemolytic Activity Towards Mammalian Red Blood Cells.* **Lin, Victor S.-Y., et al.** 2009. Small, 5. 57-62.

50. *Impacts of Mesoporous Silica Nanoparticle Size, Pore Ordering, and Pore Integrity on Hemolytic Activity.* **Haynes, Christy L. and Lin, Yu-Shen.** 2010. Journal of the American Chemical Society, 132. 4834-4842.

51. *Viscoelastic characterization of three different sol–gel derived silica gels.* **Jokinen, Mika, Györvary, Erika and Rosenholm, Jari B.** 1998. Colloids and Surfaces A: Physicochemical and Engineering Aspects, 141. 205-216.

52. *SiO2 nanoparticles biocompatibility and their potential for gene delivery and silencing.* **Malvindi, Maria Ada, et al.** 2012. Nanoscale, 4. 486-495.

53. *The toxicological mode of action and the safety of synthetic amorphous silica—A nanostructured material.* **Fruijtier-Pölloth, Claudia.** 2012. Toxicology, 294. 61-79. Potential conflict of interest as the paper was funded by Association of Synthetic Amorphous Silica Producers (ASASP).

54. **Laurie, Joyce.** Freeze Casting - A Modified Sol-Gel Process. *Dissertation, Doctor of Philosophy.* Bath : University of Bath, 1994. Available online via EThOS, ID:uk.bl.ethos.260248.

55. *Thermodynamic Properties of Organic Oxygen Compounds. XXV. Vapor Pressures and Normal Boiling Temperatures of Aliphatic Alcohols.* **Ambrose, D. and Sprake, C. H. S.** 2. 1970. Journal of Chemical Thermodynamics. From NIST Webbook: nist.webbook.org.

56. *Vapor Pressure of Mono-Poly Systems.* **Gubkov, A. N., Fermor, N. A. and Smirnov, N. I.** Leningrad : s.n., 1964. Zhurnal Prikladnoi Khimii, 37. 2204-2210. From NIST Webbook: nist.webbook.org.

57. *Observational constraints on the global atmospheric budget of ethanol.* **Naik, V., et al.** Atmospheric Chemistry and Physics, 5361-5370.

58. **Grant, David W.** *Capillary Gas Chromatography.* Chichester : John Wiley & Sons Ltd, 1996.

Appendix 1. Example calculations

The composition of the sol at any R-value ≥4 can be calculated in the following manner:

Table A 1: Constants used in sol/gel calculations

	M (g/mol)	Density ρ (g/cm^3)
TEOS	208.33	0.933
H_2O	18.02	0.997
EtOH	46.07	0.789
$Si(OH)_4$	96.1149	1.77
SiO_2	60.0843	2.196

Based on full completion of $Si(OEt)_4 + 4H_2O \longrightarrow Si(OH)_4 + 4EtOH$ and $R = \frac{n_{H_2O}}{n_{TEOS}}$ the resulting sol has the molar composition of $\underset{\frac{1}{R}}{Si(OH)_4}\quad \underset{R-\frac{4}{R}}{H_2O}\quad \underset{\frac{4}{R}}{EtOH}$.

For $n = \frac{m}{M} \rightarrow m = n * M$ and $\rho = \frac{m}{V} \rightarrow V = \frac{m}{\rho}$ results in $V = \frac{n*M}{\rho}$.

While all components contribute to the total volume V_{tot} it can be said that a single components portion is $v\%_n = \frac{V_n}{V_{tot}}$ and $V_{tot} = \sum_{i=m}^{n} V_i$.

Thus if $R = 50 \rightarrow v\%_{EtOH} = \frac{V_{EtOH}}{V_{tot}} = \frac{V_{EtOH}}{V_{EtOH}+V_{Si(OH)_4}+V_{H_2O}} = \frac{\frac{n*M}{\rho}_{EtOH}}{\frac{n*M}{\rho}_{EtOH}+\frac{n*M}{\rho}_{Si(OH)_4}+\frac{n*M}{\rho}_{H_2O}}$

The composition of the sol in moles is: $\underset{1.086}{Si(OH)_4}\quad \underset{16.628}{H_2O}\quad \underset{4.671}{EtOH}$

Appendix 2. GC parameters

Table A 2: GC parameters.

Gas chromatography	HP-6890
HS-sampler	HP-7694
Column	HP5
Column length	30 m
Column i.d.	0.32 µm
Column film thickness	0.25 µm
Serial nr.	19091J-413
Sample mass	40 mg
HS-oven temp.	105°C
HS-equiliration	3 min with shaking
HS-pressurization	0.2 min
HS-loop fill	0.2 min
HS-loop equilibration	0.05 min
HS-loop temp.	120°C
HS-transfer line temp.	140°C
Split ratio	100:1
GC-oven temp.	30°C
GC-N_2 volume flow	16 cm/s
Analyte retention time	3.40-3.45 min
FID-H_2 volume flow	40 mL/min
FID-air volume flow	450 mL/min
FID- temp.	250°C
Cycle duration	6-4 min

Appendix 3. Processing equipment

The processing equipment is illustrated in Figure A 1. The reaction vessel sits on top of a magnetic stirring platform which itself sits on top of a scale. The reaction vessel consists of two beaker glasses where the smaller one is placed inside the larger one. Two silicone tubes enter the chamber between the vessels between the lips of the vessels. The chamber is filled with water, which is circulated by a peristaltic pump through a heat exchanging coil that is placed in a water bath. A static support holds a thermometer in the reacting mixture inside the smaller beaker. A magnetic stirrer sits in the inner vessel for mixing.

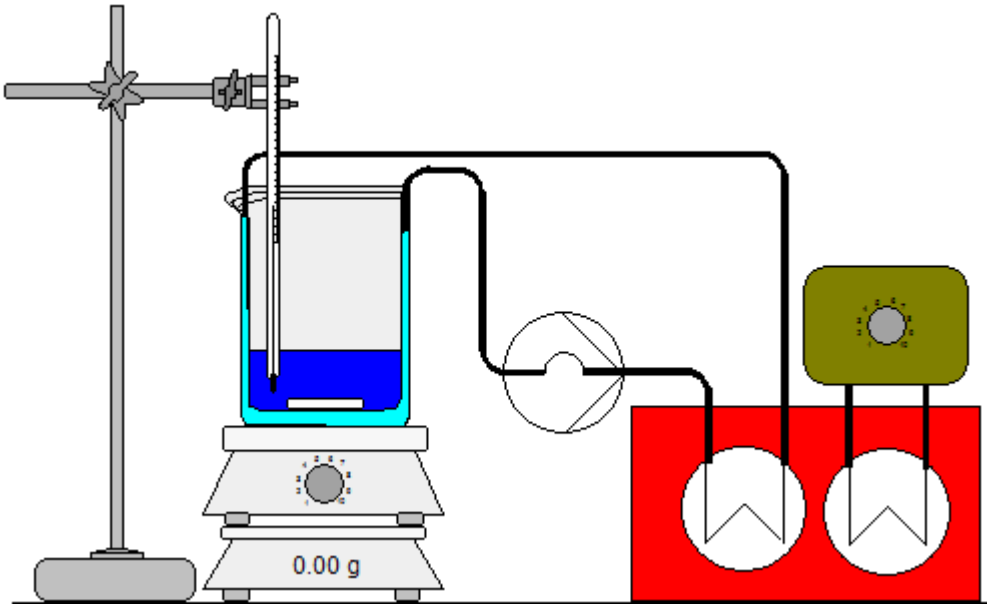

Figure A 1: Processing equipment.

Appendix 4. Data analysis

The average, standard deviation and coefficient of variation were calculated according to the following equations:

Average $\bar{x} = \frac{1}{N}\sum_{i=1}^{N} x_i$

Standard deviation $s_N = \sqrt{\frac{1}{N}\sum_{i=1}^{N}(x_i - \bar{x})^2}$

Coefficient of variation (CV%) $= \frac{s_N}{\bar{x}} * 100\%$